



Energy, Mines and
Resources Canada

Énergie, Mines et
Ressources Canada

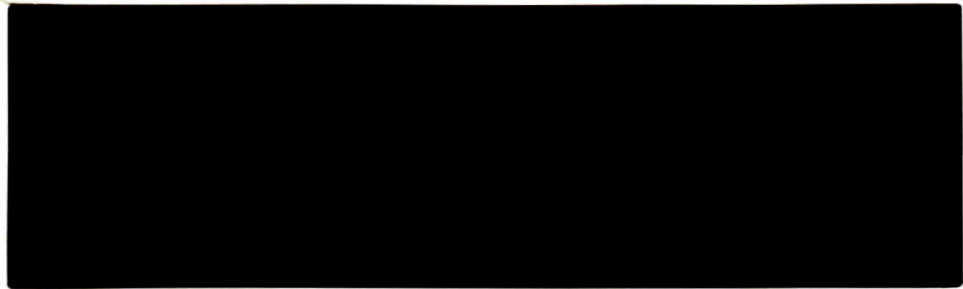
CANMET

Canada Centre for
Mineral and Energy
Technology

Centre canadien de la
technologie des
minéraux et de l'énergie

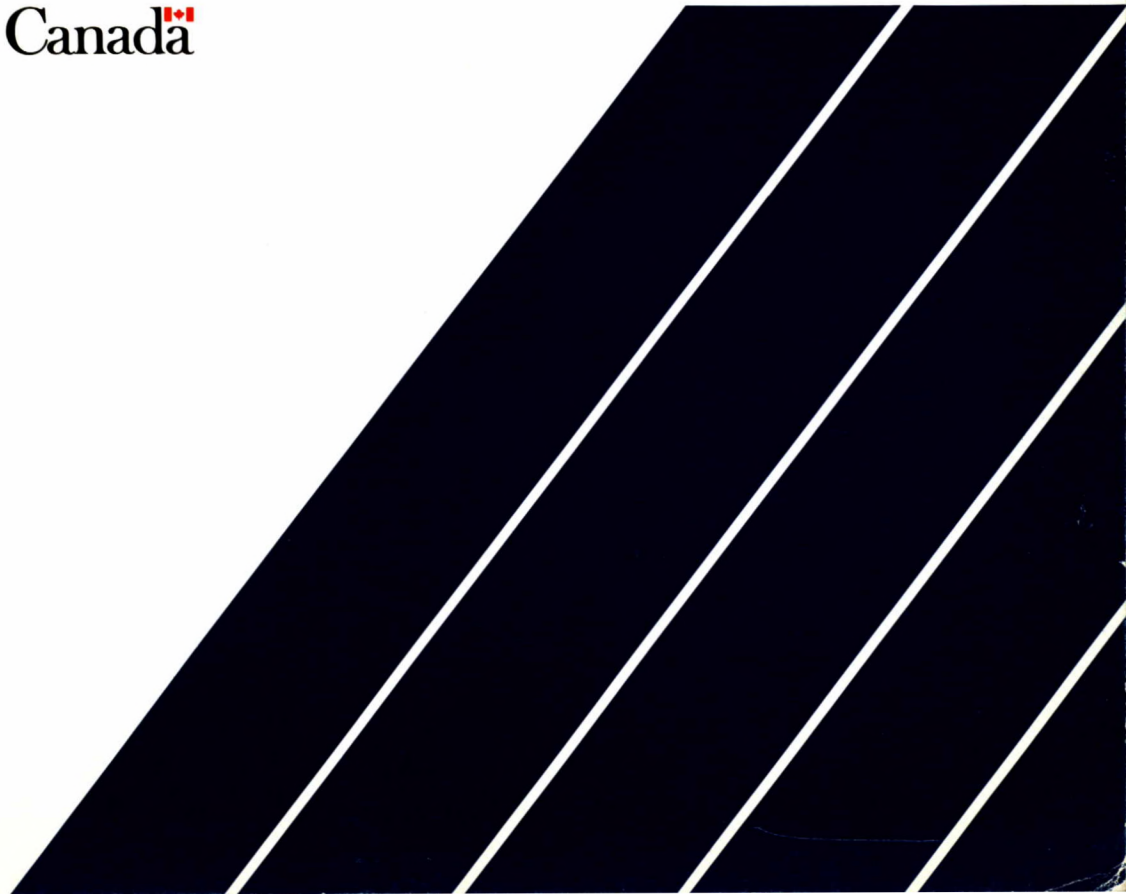
**Mining
Research
Laboratories**

**Laboratoires
de recherche
minière**



Canada^{ca}

MRL 88-112 (TR)



1-7987793

HIGH TEMPERATURE TRIAXIAL TESTS ON ROCK
SAMPLES FROM BOREHOLES 209-021-SV1 AND
209-030-DIL1, LAC DU BONNET, MANITOBA

J.S.O. Lau, R. Jackson and B. Gorski

MRL 88-112(TR)

61 pp.

HIGH TEMPERATURE TRIAXIAL TESTS ON ROCK SAMPLES FROM
BOREHOLES 209-021-SV1 AND 209-030-DIL1, LAC DU BONNET, MANITOBA

by

J.S.O. Lau¹, R. Jackson² and B. Gorski³

ABSTRACT

A series of ambient and high temperature triaxial tests were conducted on grey granitic core samples obtained from Boreholes 209-021-SV1 and 209-030-DIL1 located at the 240 level of Atomic Energy of Canada Limited's Underground Research Laboratory (URL). Nine sets of tests at three confining pressures (3.5, 17.0 and 35.0 MPa) and three temperatures (ambient, 75° and 125° C) were performed. The purpose of these tests is to investigate the thermal-mechanical properties of the rock mass at the URL site. The failure deviator stress and the total axial strain of each of the specimens tested were recorded. Both the tangent Young's modulus and the pseudo Young's modulus were used to describe the elastic properties of the rock samples. The strength properties were expressed in terms of the Hoek and Brown failure criterion. The effects of temperature on the mechanical and elastic properties of the rock samples were discussed.

¹Geotechnical Engineer, Atomic Energy of Canada Limited, on attachment to CANMET, Energy, Mines and Resources Canada, Ottawa, Ontario.

²Research Officer, Canadian Mine Technology Laboratory, Mining Research Laboratories, CANMET, Energy, Mines and Resources Canada, Ottawa, Ontario.

³Rock Mechanics and Development Technologist, Canadian Mine Technology Laboratory, Mining Research Laboratories, CANMET, Energy, Mines and Resources Canada, Ottawa, Ontario.

Keywords: thermal-mechanical, dynamic, elastic, strength, confining pressure, temperature, deviator stress, strain, Young's modulus

ESSAIS TRIAXIAUX HAUTE TEMPÉRATURE SUR DES ÉCHANTILLONS
DE ROCHE PROVENANT DES TROUS DE SONDAGE
209-021-SV1 ET 209-030-DIL1 À LAC DU BONNET, MANITOBA

par

J.S.O. Lau¹, R. Jackson² et B. Gorski³

RÉSUMÉ

Une série d'essais triaxiaux sous température ambiante et hautes températures ont été réalisés sur des carottes de granite gris prélevées dans les trous de sondage 209-021-SV1 et 209-030-DIL1 forés au niveau 240 du Laboratoire de recherche souterrain (URL) de L'Énergie atomique du Canada Limitée. Neuf séries d'essais ont été réalisés à trois différentes pressions de confinement (3.5, 17.0 et 35.0 MPa) et trois différentes températures (ambiante, 75° et 125° C). Ces essais ont pour objectif d'analyser les propriétés thermo-mécaniques du massif rocheux où se trouve le URL. La contrainte déviatrice de rupture et la déformation axiale totale ont été enregistrées dans chacune des carottes. Le module de Young tangent et le pseudo-module de Young ont été utilisés pour décrire les propriétés élastiques des échantillons. Leur résistance a été exprimée en fonction des critères de rupture de Hoek et de Brown. Les effets de la température sur les propriétés mécaniques et élastiques des carottes sont traités.

¹Ingénieur géotechnique de L'Énergie atomique de Canada Limitée, affecté à CANMET, Énergie, Mines et Ressources Canada, Ottawa, Ontario.

²Agent de recherche, Laboratoire canadien de technologie minière, Laboratoires de recherche minière, CANMET, Énergie, Mines et Ressources Canada, Ottawa, Ontario.

³Technicien, Développement et mécanique des roches, Laboratoire canadien de technologie minière, Laboratoires de recherche minière, CANMET, Énergie, Mines et Ressources Canada, Ottawa, Ontario.

Mots-clé: thermique-mécanique, dynamique, élastique, résistance, pression de confinement, température, contrainte déviatrice, déformation, module de Young.

CONTENTS

	<u>Page No.</u>
Abstract	i
Résumé	ii
1. Introduction	1
2. Sampling and specimen preparation	2
3. Dynamic elastic properties	2
4. Test apparatus and procedure	4
5. Triaxial testing program	4
6. Results and discussion	5
6.1 Test results	5
6.2 Deviator stress and strain at failure	5
6.3 Effect of temperature on deviator stress and strain at failure	6
6.4 Tangent Young's modulus	6
6.5 Effect of temperature on tangent Young's modulus	7
6.6 Pseudo Young's modulus	8
6.7 Effect of temperature on pseudo Young's modulus	8
6.8 Strength properties	8
6.9 Effect of temperature on strength properties	11
7. Conclusions	12
8. Recommendations	13
Acknowledgements	14
References	14
Appendix A	39

1. Introduction

A joint project has been undertaken by Canada Centre for Mineral and Energy Technology (CANMET) and Atomic Energy of Canada Limited (AECL) to investigate the thermal-mechanical properties of rock samples from the site of AECL's Underground Research Laboratory (URL) located near to Lac du Bonnet, Manitoba. An understanding of the stability and deformability of the rock mass at high temperature and pressure is an essential component of the Canadian Nuclear Fuel Waste Management Program for the safe, long term disposal of high level nuclear wastes in a vault deep in plutonic rock.

The effects of pressure and temperature on the mechanical behaviour of some rock samples from the URL site have been described in detail by Annor et al. (1981), Jackson (1984), Annor and Jackson (1985) and Annor and Jackson (1987). The core samples they tested were obtained from Borehole URL-6 between the depths of 225.10 and 259.26 m. Their pressure and temperature paths were to heat the specimens to the predetermined temperatures first and then apply the confining pressures. They observed that the triaxial compressive strengths of the tested samples increased with increasing confining pressure and decreased with increasing temperature. The greatest decrease occurred at the low confining pressure of 3.5 MPa. At higher confining pressure levels, the effect of temperature on the strength of the rock became minimal. They also reported some decrease in the modulus of elasticity with increasing temperature at low confining pressures.

A different procedure was employed by Lau et al. (1988), to test core samples obtained from Borehole URL-5 between the downhole lengths of 268.84 and 277.57 m (depth of 260.32 to 268.66 m). Using a MTS 815 Rock Mechanics Test System, the confining pressures were applied first and then the specimens were heated to the test temperatures. The test results indicated that the failure deviator stress increased with increasing confining pressure and decreased when the temperature was raised from 23° to 100° C at the confining pressures of 3.5 and 17.0 MPa. However, at the high confining pressure of 35.0 MPa, no such a decrease was observed. Results obtained at the test temperature of 200° C was inconclusive, although a reduction in the failure deviator stress was observed in a few tests. Temperature was found to have no effect on the modulus of elasticity at the confining pressure of 17.0 and 35.0 MPa, but at the low confining pressure of 3.5 MPa, the modulus decreased with increasing temperature at stress levels below 75% of the failure deviator stress.

A program was initiated early in 1988 to conduct triaxial tests at the temperatures of 75° and 125° C to better define the effects of temperature on rock properties near

the anticipated cannister temperature of 100° C (Baumgartner, 1986). This is also the range in which most of the changes in the strength and elastic properties of the rock samples were found to occur in previous studies. This report presents the results of the testing program on samples obtained from Boreholes 209-021-SV1 and 209-030-DIL1.

2. Sampling and specimen preparation

Samples were prepared from NQ cores obtained in the Underground Research Laboratory at the 240 level, from Boreholes 209-021-SV1 and 209-030-DIL1. The rock is a massive, grey, medium to coarse grained granite, composed of quartz, K-feldspar, plagioclase and biotite.

Cylindrical test specimens were prepared in accordance to the procedure described in the Pit Slope Manual Supplement 3-5 (Gyenge and Ladanyi, 1977) and the method suggested by the International Society for Rock Mechanics (Brown, 1981). Specimens were first cut slightly larger than their final dimensions from the core samples by means of a water-cooled diamond saw. Then, using a double lapper, the end surfaces of each specimen were ground flat to 0.025 mm to ensure that the end surfaces were parallel to each other and perpendicular to the axis of the specimen.

After the specimens had been prepared, they were oven dried, weighed and measured. The dimensions and bulk densities of the specimens are shown in Table 1. The final dimensions of the specimens for these tests varied from 44.86 to 45.11 mm in diameter and 95.47 to 117.16 mm in length, with length to diameter ratios ranging from 2.1 to 2.6.

3. Dynamic elastic properties

Compression and shear wave velocity measurements were carried out on the specimens prior to conducting the high temperature triaxial tests. The testing apparatus consisted of pulsing and sensing heads, a pulse generator and an oscilloscope. For a detailed description of the apparatus and an outline of the test method, the reader is referred to the Instruction Manual - Sonic Velocity Equipment (Terrametric, 1980) and the Pit Slope Manual Supplement 3-2 (Gyenge and Herget, 1977). The velocity measurements offered a method of estimating various mechanical properties of the rock samples non-destructively prior to actual testing.

The compression and shear wave velocities of each specimen were determined by dividing the length of the specimen by the pulse-travel times through the specimen of the compression wave and the shear wave respectively. The dynamic elastic constants were then computed by using the following equations.

Dynamic Young' modulus of elasticity:

$$E_u = \frac{\rho V_s^2 (3V_p^2 - 4V_s^2)}{V_p^2 - V_s^2} \quad (1)$$

where E_u = dynamic Young's modulus of elasticity

V_p = compression wave velocity

V_s = shear wave velocity

ρ = bulk density

Dynamic shear modulus:

$$G_u = \rho V_s^2 \quad (2)$$

where G_u = dynamic shear modulus

Dynamic Poisson's ratio:

$$\nu_u = \frac{V_p^2 - 2V_s^2}{2(V_p^2 - V_s^2)} \quad (3)$$

where ν_u = dynamic Poisson's ratio

The compression and shear wave velocities, dynamic Young's modulus, dynamic shear modulus and dynamic Poisson's ratio determined for each of the specimens are shown in Table 1. The dynamic Young's moduli of the rock samples were found to vary from 42.71 to 57.44 GPa with a mean value of 50.33 GPa (standard deviation = 4.43 GPa). The dynamic shear moduli varied from 16.88 to 24.59 GPa with a mean value of 20.38 GPa (standard deviation = 2.01 GPa). The dynamic Poisson's ratios varied from 0.17 to 0.29 with a mean value of 0.24 (standard deviation = 0.03).

4. Test apparatus and procedure

The triaxial apparatus used to carry out these tests was a MTS 815 Rock Mechanics Test System consisting of a load frame, hydraulic power supply, triaxial cell, confining pressure subsystem, test controller, data display, function generator, hydraulic controller, micro-console, test processor, temperature controller and DEC micro PDP 11/73 computer. The triaxial cell is rated up to 150 MPa and 200° C and equipped with a 2.22 MN rated load cell, heater, heat shroud, thermocouples and three linear variable differential transducers (LVDTs) for the measurement of axial strain. For a detailed description of the MTS system and its operation, the reader is referred to the MTS Operation Manual (MTS Systems Corp., 1986) and CANMET Division Report MRL 87-33(INT) (Gorski, 1987).

The test stack for the rock specimen was assembled using the procedure outlined in CANMET Division Report MRL 88-90(TR) (Lau et al., 1988). In the high temperature triaxial tests, the confining fluid pressure and the axial load were raised simultaneously to the test level and then the confining fluid was heated at a rate of 1° C per minute until the test temperature was reached. A soak time of one hour was allowed to ensure that the specimen also reached the test temperature.

All specimens were loaded at a constant rate of 1 kN per second under computer control. Signals from the load cell and the three LVDTs were scanned by the computer every second. The signals were converted to engineering units and measurements from the LVDTs were corrected for end platen compression. The data were stored on hard disk in the micro PDP 11/73 computer and later transferred to the VAX computer for data analysis and plotting.

After the test had been completed, the confining fluid was cooled down, drained and the assembly dismantled. The failure characteristics of the specimen was noted and the angle between the failure plane and the axis of the specimen was measured.

5. Triaxial testing program

The triaxial testing program consisted of nine sets of tests. Three sets were conducted at each of the following temperatures: the ambient room temperature, 75° and 125° C. At each temperature, the tests were carried out under three different confining pressure conditions, namely, 3.5, 17.0 and 35.0 MPa respectively. Testing took place at Mining Research Laboratories, CANMET, Energy, Mines and Resources

Canada in Ottawa in October, 1988. A total of 18 tests were performed and the testing program is summarized in Table 2.

6. Results and discussion

6.1 Test results

The purpose of the high temperature triaxial tests was to determine the behaviour of the rock samples under high temperature conditions in order to compare it with the behaviour under ambient temperature condition. Table 2 summarizes the total axial strain, failure deviator stress, tangent Young's modulus and pseudo Young's modulus at 50% failure deviator stress, failure angle and failure characteristics of each specimen for the tests conducted under ambient and high temperature conditions. The effects of temperature on the strength and elastic properties of the rock samples will be discussed in the following subsections.

Deviator stress versus axial strain curves for all tests are illustrated in Appendix A. These curves were plotted using the computer DATAPLOT fitting operation. A cubic spline fit was used for analysis which employed a third degree equation model of the form:

$$\sigma = a_0 + a_1\varepsilon + a_2\varepsilon^2 + a_3\varepsilon^3 \quad (4)$$

where σ = stress

ε = strain

and a_0 , a_1 , a_2 and a_3 are coefficients

Note that the axial strain was computed by averaging the axial strain data obtained from the three LVDTs.

6.2 Deviator stress and strain at failure

Both the failure deviator stress and the total axial strain at failure increased as the confining pressure increased at all three test temperatures (see Table 2 and Fig. 1).

At the ambient room temperature, the mean failure deviator stress increased from 423 MPa at the confining pressure of 17.0 MPa to 552 MPa at the confining pressure of

35.0 MPa. The mean total axial strain also increased from 0.675 to 0.877. Results from the two tests (Sample Numbers A044 and A054) conducted at the confining pressure of 3.5 MPa and one of the tests (Sample Number A066) carried out at the confining pressure of 17.0 MPa were not used in this analysis because of the presence of large quartz inclusions in those specimens, which greatly reduced the strength of the rock.

At the temperature of 75° C, the mean failure deviator stress increased from 268 MPa to 401 MPa to 513 MPa and the mean total axial strain at failure increased from 0.446 to 0.667 to 0.835 as the confining pressure increased from 3.5 to 17.0 to 35.0 MPa.

At 125° C, as the confining pressure increased from 3.5 to 17.0 to 35.0 MPa, the mean failure deviator stress increased from 243 MPa to 391 MPa to 507 MPa and the mean total axial strain at failure increased from 0.440 to 0.636 to 0.818.

6.3 Effect of temperature on deviator stress and strain at failure

One of the main objectives of these tests is to study the effect of temperature on the strength of the rock. Results from the tests (see Fig. 1 and Table 2) showed that both the failure deviator stress and the total axial strain at failure decreased as the temperature increased. The decrease was more significant when the temperature was raised from the ambient room temperature to 75° C.

At the confining pressure of 3.5 MPa, the mean failure deviator stress decreased from 268 MPa at the temperature of 75° C to 243 MPa at the temperature of 125° C. The mean total axial strain at failure also decreased from 0.446 to 0.440.

At the confining pressure of 17.0 MPa, the mean failure deviator stress decreased from 423 MPa to 401 MPa to 391 MPa and the mean total axial strain decreased from 0.675 to 0.667 to 0.636 as the temperature increased from ambient room temperature to 75° to 125° C.

At the confining pressure of 35.0 MPa, as the temperature was raised from 22° to 75° to 125° C, the mean failure deviator stress decreased from 552 MPa to 513 MPa to 507 MPa and the mean total strain at failure decreased from 0.877 to 0.835 to 0.818.

6.4 Tangent Young's modulus

Tangent Young's moduli of the rock samples were computed at stress levels corresponding to 10%, 20%, 30%, 40%, 50%, 60%, 70%, 80%, 90% and 100% of the failure

deviator stress, $(\sigma_1 - \sigma_3)_f$, and are presented in Table 3. For each sample, the tangent modulus at each stress level was computed by solving the third degree equation (Equation 4) representing the stress-strain curve and substituting the strain value into the derivative of the equation. The tangent Young's modulus was plotted against the normalized deviator stress for the three temperature conditions (ambient room temperature, 75° and 125° C) in Figures 2, 3 and 4 respectively. The normalized deviator stress was computed by dividing the deviator stress by the failure deviator stress.

Under all three temperature conditions, the tangent modulus increased as the normalized deviator increased at the confining pressure of 3.5 MPa until approximately $0.5(\sigma_1 - \sigma_3)_f$ was reached and then decreased until failure. At the confining pressure of 17.0 MPa, the tangent modulus increased slowly as the normalized deviator stress increased from zero to approximately $0.2(\sigma_1 - \sigma_3)_f$ and then decreased slowly with increasing stress. At the high confining pressure of 35.0 MPa, the tangent modulus decreased slowly with increasing deviator stress.

In the modulus-stress plots, the tangent modulus started to decrease more rapidly at approximately $0.5(\sigma_1 - \sigma_3)_f$ under all temperature and confining pressure conditions. Note that all these plots (see Figs. 2, 3 and 4) join at approximately $0.6(\sigma_1 - \sigma_3)_f$, indicating that the increase of confining pressure had no effect on the tangent modulus at stress levels above $0.6(\sigma_1 - \sigma_3)_f$. Below $0.6(\sigma_1 - \sigma_3)_f$, an increase in the confining pressure resulted in an increase in the tangent modulus, especially at low stress levels. The increase was particularly pronounced when the confining pressure was raised from 3.5 MPa to 17.0 MPa, indicating that some stress relaxation might have occurred, resulting in higher crack porosity, larger deformations and lower modulus values at the low confining pressure of 3.5 MPa.

6.5 Effect of temperature on tangent Young's modulus

The variation of the tangent Young's modulus with temperature at the confining pressures of 3.5, 17.0 and 35.0 MPa are shown in Figures 5, 6 and 7 respectively. Results of tests conducted at the low confining pressure of 3.5 MPa were inconsistent. There was an increase in the tangent modulus when the temperature was increased from the ambient room temperature to 75° C, but a decrease when the temperature was raised from 75° to 125° C. This inconsistency may be due to the presence of large inclusions of quartz in the two specimens (209-021-SV1-0.44 and 209-021-SV1-0.54) tested at the ambient room temperature, resulting in lower failure deviator stresses and lower modulus values for those two specimens. At the confining pressures of 17.0 MPa and 35.0 MPa,

no significant change in the tangent modulus was observed at any stress level as the temperature increased from the ambient room temperature to 75° and to 125° C.

6.6 Pseudo Young's modulus

Actual stress-strain curves for rock are seldom linear. However, for modelling purposes, these nonlinear curves may be idealized as a series of straight lines joining points corresponding to stress levels of 0.0, 0.1, 0.2, 0.3, 0.4, 0.5, 0.6, 0.7, 0.8, 0.9 and 1.0 times the failure deviator stress. The slope of the linear stress-strain curve during each stress interval is defined as the pseudo Young's modulus. The pseudo Young's moduli of the rock samples are presented in Table 4. In general, the pseudo modulus was lower than the tangent modulus at stress levels below $0.5(\sigma_1 - \sigma_3)_f$, but higher at stress levels above $0.5(\sigma_1 - \sigma_3)_f$.

The plots of the pseudo Young's modulus versus the normalized deviator stress of the rock samples tested at the ambient room temperature, 75° and 125° C are shown in Figures 8, 9 and 10 respectively. Their patterns are very similar to those of the tangent Young's modulus (see Figs. 2, 3 and 4). These plots also join at approximately $0.6(\sigma_1 - \sigma_3)_f$, indicating that the increase of confining pressure also had no effect on the pseudo Young's modulus at stress levels above $0.6(\sigma_1 - \sigma_3)_f$.

6.7 Effect of temperature on pseudo Young's modulus

To study the effect of temperature on the pseudo Young's modulus, the pseudo Young's modulus was plotted against the normalized deviator stress for each of the tests conducted at the confining pressures of 3.5, 17.0 and 35.0 MPa in Figures 11, 12 and 13 respectively. The same patterns as those exhibited by the tangent Young's modulus (see Figs. 5, 6 and 7) were observed. The results of the tests conducted at the confining pressure of 3.5 MPa were also inconsistent for the same reason. At the confining pressures of 17.0 and 35.0 MPa, an increase of temperature from the ambient room temperature to 75° and to 125° C resulted in no significant change in the pseudo modulus.

6.8 Strength properties

The strength properties of the intact rock material can be expressed in terms of the Mohr-Coulomb and Hoek and Brown failure criteria.

Using the Mohr-Coulomb failure criterion (Goodman, 1980), the major principal stress at failure is given as follows:

$$\sigma_1 = \sigma_c + \sigma_3 \tan^2(45^\circ + \phi/2) \quad (5)$$

where σ_1 = major principal stress at failure
 σ_c = uniaxial compressive strength
 σ_3 = minor principal stress (confining pressure)
 ϕ = angle of internal friction

This criterion yields a curved failure envelope.

Using the Hoek and Brown failure criterion (Hoek and Brown, 1980), the relationship between the principal stresses associated with the failure of rock are expressed as follows:

$$\sigma_1 = \sigma_3 + \sqrt{m\sigma_c\sigma_3 + s\sigma_c^2} \quad (6)$$

where σ_1 = major principal stress at failure
 σ_3 = minor principal stress applied to the rock sample
 σ_c = uniaxial compressive strength of the intact rock material
in the specimen
 m and s are constants

The values of m and s depend on the properties of the rock and the extent to which the rock has been broken before being subjected to the stresses σ_1 and σ_3 . For intact rock, $s = 1$, and the uniaxial compressive strength σ_c and the material constant m can be computed by using the following equations:

$$\sigma_c^2 = \frac{\sum y_i}{n} - \left[\frac{\sum x_i y_i - \frac{\sum x_i \sum y_i}{n}}{\sum x_i^2 - \frac{(\sum x_i)^2}{n}} \right] \frac{\sum x_i}{n} \quad (7)$$

$$m = \frac{1}{\sigma_c} \left[\frac{\sum x_i y_i - \frac{\sum x_i \sum y_i}{n}}{\sum x_i^2 - \frac{(\sum x_i)^2}{n}} \right] \quad (8)$$

where $x = \sigma_3$

$$y = (\sigma_1 - \sigma_3)^2$$

n = total number of data pairs x_i and y_i

The coefficient of determination r^2 is given by:

$$r^2 = \frac{\left[\sum x_i y_i - \frac{\sum x_i \sum y_i}{n} \right]^2}{\left[\sum x_i^2 - \frac{(\sum x_i)^2}{n} \right] \left[\sum y_i^2 - \frac{(\sum y_i)^2}{n} \right]} \quad (9)$$

The closer the value of r^2 is to 1.00, the better the fit of Equation 6 to the triaxial test data is.

Hoek and Brown also suggest that the relationship between the shear and normal stresses (τ and σ) and the principal stresses can be expressed as:

$$\sigma = \sigma_3 + \frac{\tau_m^2}{\tau_m + m\sigma_c/8} \quad (10)$$

$$\tau = (\sigma - \sigma_3) \sqrt{1 + m\sigma_c/4\tau_m} \quad (11)$$

where $\tau_m = \frac{1}{2}(\sigma_1 - \sigma_3)$

The failure envelopes for the rock samples were developed using Equations 10 and 11. Since no uniaxial compressive strength σ_c of the rock at elevated temperature was available, the values of σ_c and m , used in Equations 10 and 11, had to be computed first, using Equations 7 and 8. The values of r^2 were also computed, using Equation 9. These values are shown in Table 5. The coefficient of determination r^2 ranged from 0.9483 to 0.9870, indicating that the fit of Equation 6 to the triaxial data was good. The values of σ_c and m were substituted into Equations 10 and 11 to generate a series of σ and τ data for the development of the failure envelopes.

The Mohr circles and the failure envelopes for the rock samples tested at the ambient room temperature, 75° and 125° C were plotted in Figures 14, 15 and 16 respectively. Note that only the average Mohr circle was plotted for each set of tests

conducted under the same conditions of confining pressure and temperature. It can be seen that the failure envelopes developed using Equations 10 and 11 fit very well with the Mohr circles.

The value of the material constant m obtained for the rock samples tested at the ambient room temperature is 28.28. The mean values of m for unheated Lac du Bonnet grey granitic samples reported by Annor and Jackson (1987) and Lau et al. (1988) are 29.9 and 31.88 respectively. The m values for granitic rocks established by Hoek and Brown (1980) range from 20.8 to 32.8, indicating a good agreement between the m value for the unheated granitic samples obtained in these tests and those reported in the published literature.

The angles of internal friction and the cohesive strength of the rock samples were measured in Figures 14, 15 and 16 and are shown in Table 6. The angle of internal friction decreased but the cohesive strength increased with increasing confining pressure at all temperatures. At the ambient room temperature, the angle of internal friction decreased from 55° to 48° and the cohesion increased from 43 to 66 MPa, as the confining pressure increased from 17.0 to 35.0 MPa. At the temperatures of 75° and 125° C, the angle of internal friction decreased from 58° to 54° to 47° and from 59° to 55° to 48° respectively, and the cohesion increased from 36 to 43 to 66 MPa and from 30 to 39 to 62 MPa respectively, as the confining pressure increased from 3.5 to 17.0 to 35.0 MPa.

6.9 Effect of temperature on strength properties

All three failure envelopes for the three test temperatures were plotted in Figure 17 to study the effect of temperature on the strength properties of the rock samples. It can be seen that there was a slight decrease in the strength when the temperature was raised from the ambient room temperature to 75° C. However, no significant change in the failure envelope was observed when the temperature was raised from 75° to 125° C.

The material constant m computed for the heated rock samples is 26.31 at 75° C and 31.27 at 125° C. These values are more realistic than those m values (37.22 and 73.50 at 100° C and 35.39 and 47.32 at 200° C) obtained from tests conducted on grey granitic samples from Borehole URL-5 (Lau et al., 1988), and compared very well with the m values (30.06 at 100° and 37.56 at 200°) for Lac du Bonnet pink granitic samples reported by Annor and Jackson (1987). However, the effect of temperature on the material constant m is still not clear. More test data, especially uniaxial compressive strength data on heated samples, are required to better estimate the m value at high temperature in order to compare it with its value at ambient room temperature.

The results show that there was no significant change in the angle of internal friction, but a slight decrease in the cohesive strength of the samples when the temperature was raised from 75° to 125° C.

7. Conclusions

The results of these tests have provided some insight into the behaviour of the grey granite at the 240 level of the AECL Underground Research Laboratory under both ambient and high temperature conditions. The results also provide additional data for the study of the thermal-mechanical properties of the granitic rock at the URL site. From the results, the following conclusions can be made:

The mean values of the dynamic Young's modulus, dynamic shear modulus and Poisson's ratio of the rock samples were found to be 50.33 GPa, 20.38 GPa and 0.24 respectively.

Both the failure deviator stress and the total strain at failure of the rock specimens increased as the confining pressure increased at ambient room temperature and at the high temperatures of 75° and 125° C.

The failure deviator stress and the total axial strain at failure decreased with increasing temperature. This decrease was most pronounced when the temperature was raised from the ambient room temperature to 75° C.

The tangent Young's modulus and the pseudo Young's modulus were used to describe the elastic properties of the rock samples. The pseudo Young's modulus is more useful for finite element analysis. In general, the pseudo Young's modulus was lower than the tangent Young's modulus at stress levels below approximately $0.5(\sigma_1 - \sigma_3)_f$, but higher than the tangent modulus at stress levels above approximately $0.5(\sigma_1 - \sigma_3)_f$.

At stress levels below approximately $0.6(\sigma_1 - \sigma_3)_f$, both the tangent Young's modulus and the pseudo Young's modulus increased with increasing confining pressure. The increase was more significant at low stress levels and particularly pronounced when the confining pressure was raised from 3.5 to 17.0 MPa, indicating that some stress relaxation might have occurred in the rock samples. At stress levels above approximately $0.6(\sigma_1 - \sigma_3)_f$, the increase in the confining pressure resulted in no significant change in the modulus values.

The results show that in the temperature range of 19° to 125° C, the temperature had no effect on the tangent Young's modulus and the pseudo Young's modulus.

The strength properties of the rock samples were expressed in terms of the Hoek and Brown failure criterion. The values of the material constant m were found to be 28.28 for the unheated samples, 26.31 for samples tested at 75° C and 31.27 for samples tested at 125° C. There is a good agreement between these values and the m values reported in published literature for Lac du Bonnet granite and other granitic rocks. However, the effect of temperature on the value of m is still not clear.

The angle of internal friction appeared to be relatively insensitive to the increase in temperature. However, there was a slight decrease in the cohesive strength of the rock samples when the temperature was raised from 75° to 125° C.

8. Recommendations

The Hoek and Brown failure criterion for rocks has been used to study the strength properties of the URL rock samples. The absence of the high temperature uniaxial compressive and tensile strength test data has created some uncertainty in the determination of the material constant m for heated URL rock samples. Since the techniques to conduct the uniaxial compression test and tension test on heated rock samples do not exist, it is strongly recommended that some high temperature triaxial tests at very low confining pressure to be carried out to provide some data close to the uniaxial compression test data.

All the URL rock samples used in these high temperature triaxial tests and previous tests are samples obtained from the upper 270 m of the rock mass at the URL site. Further testing should be performed on samples obtained at greater depths, especially at depths closely associated with the second operating level of the URL, to provide data to study the effect of high temperature as well as the effect of stress relaxation on rock samples at great depth. Boreholes URL-1, URL-2, URL-5 and URL-12 could provide such samples.

At present, only two types of rock, namely, the grey granite and the pink granite, have been tested at high temperature. High temperature triaxial tests should be carried out on other types of rock found at the URL site to provide data to better model the response of the rock mass to changes in stress and temperature.

The scale effects on the thermal-mechanical properties of the URL rock samples should also be studied in order to better relate the laboratory determined thermal-mechanical properties to in situ conditions.

Acknowledgements

The authors wish to express their thanks to S.M. Grinnell for carrying out the compression and shear wave measurements.

References

- Annor, A., Miles, P., Kapeller, F. and Larocque, G. (1981), "High temperature and pressure triaxial compression tests on rock samples from Pinawa and the Creighton Mine", Atomic Energy of Canada Limited Technical, Record TR-158, 51 p.
- Annor, A. and Jackson, R. (1985), "Mechanical properties of rock samples from the Lac du Bonnet Batholith, Manitoba", Division Report M&ET/MRL 85-41(TR), CANMET, Energy, Mines and Resources Canada, 101 p.
- Annor, A. and Jackson, R. (1987), "Mechanical, thermomechanical and joint properties of rock samples from the Lac du Bonnet Batholith, Manitoba", in Geotechnical studies at Whiteshell Research Area (RA-3) (edited by Katsube, T.J. and Hume, J.P.), Division Report MRL 87-52(TR), CANMET, Energy, Mines and Resources Canada, 232 p.
- Baumgartner, P. (1986), "The used fuel disposal centre study: study plan and technical specifications", in Proceedings of the 2nd International Conference on Radioactive Waste Management, Winnipeg, Manitoba, Canada, September 7-11, 1986, p. 427-431.
- Brown, E.T. (1981), "Rock characterization testing and monitoring, ISRM suggested methods", International Society for Rock Mechanics, the Commission on Testing Methods, Pergamon, 211 p.
- Goodman, R.E. (1980), "Introduction to Rock Mechanics", John Wiley and Sons, Inc., New York, 478 p.
- Gorski, B. (1987), "Post-failure uniaxial strength determinations using a servo-hydraulic test system", Division Report MRL 87-33(INT), CANMET, Energy, Mines and Resources Canada, 77 p.
- Gyenge, M. and Herget, G. (1977), "Pit slope manual supplement 3-2 - laboratory tests for design parameters", CANMET, CANMET Report 77-26, 74 p.
- Gyenge, M. and Ladanyi, B. (1977), "Pit slope manual supplement 3-5 - sampling and specimen preparation", CANMET, CANMET Report 77-29, 30 p.

Hoek, E. and Brown, E.T. (1980), "Underground excavations in rock", The institution of Mining and Metallurgy, London, 527 p.

Jackson, R. (1984), "Summary of mechanical properties of Lac du Bonnet and Eye-Dashwa specimens", Division Report MRP/MRL 84-85(TR), CANMET, Energy, Mines and Resources Canada, 48 p.

Lau, J.S.O., Jackson, R. and Gorski, B. (1988), "High temperature triaxial tests on rock samples from Borehole URL-5, Lac du Bonnet, Manitoba", Division Report MRL 88-90(TR), CANMET, Energy, Mines and Resources Canada, 86 p.

MTS Systems Corporation (1986), "Operation manual for 815 rock mechanics test systems", MTS Systems Corp., Minneapolis, Minnesota, U.S.A.

Terrametrics (1980), "Instruction manual - sonic velocity equipment", Terrametrics, Inc., Golden, Colorado, U.S.A., 17 p.

Table 1. Dimensions, densities and dynamic elastic properties of rock samples

Specimen identification	Length (mm)	Diameter (mm)	Bulk density (g/cc)	P-wave velocity (km/s)	S-wave velocity (km/s)	Dynamic Young's modulus (GPa)	Dynamic shear modulus (GPa)	Dynamic Poisson's ratio
209-021-SV1-0.44	96.53	44.99	2.634	4.858	2.728	49.768	19.597	0.27
209-021-SV1-0.54	96.98	44.97	2.615	4.930	2.687	48.668	18.883	0.29
209-021-SV1-0.66	95.47	44.99	2.634	4.653	2.728	48.548	19.609	0.24
209-021-SV1-0.76	97.09	45.01	2.639	5.132	2.886	55.777	21.983	0.27
209-021-SV1-0.89	115.77	45.00	2.641	4.830	3.051	57.435	24.590	0.17
209-021-SV1-1.01	117.16	45.02	2.639	4.919	2.997	57.117	23.707	0.21
209-021-SV1-1.13	106.87	45.02	2.643	4.777	2.784	50.916	20.482	0.24
209-021-SV1-1.24	109.63	45.00	2.647	4.934	2.924	55.648	22.635	0.23
209-021-SV1-1.35	107.38	45.00	2.650	4.897	2.861	53.831	21.691	0.24
209-021-SV1-1.47	111.74	45.03	2.641	4.761	2.840	52.146	21.307	0.22
209-021-SV1-1.58	98.94	45.05	2.644	4.663	2.726	48.748	19.653	0.24
209-021-SV1-1.69	96.32	45.10	2.634	4.823	2.838	52.409	21.214	0.24
209-021-SV1-1.79	100.13	45.11	2.640	4.775	2.752	50.027	19.988	0.25
209-030-DIL1-8.30	104.67	44.94	2.639	4.367	2.652	44.832	18.559	0.21
209-030-DIL1-8.60	98.58	44.86	2.647	4.467	2.525	42.706	16.878	0.27
209-030-DIL1-9.60	102.44	44.94	2.640	4.402	2.655	45.181	18.604	0.21
209-030-DIL1-9.70	105.46	44.98	2.631	4.503	2.647	45.572	18.436	0.24
209-030-DIL1-9.90	102.36	44.98	2.638	4.535	2.680	46.682	18.951	0.23

Table 2. Results of ambient temperature and high temperature triaxial tests

Specimen	Sample Number	Length (mm)	Diameter (mm)	Confining Pressure (MPa)	Temp. (deg C.)	Total Axial Strain (%)	Failure Deviator Stress (MPa)	Tangent Young's Modulus (GPa)	Pseudo Young's Modulus (GPa)	θ (deg)	Failure characteristics
209-021-SV1-0.44	A044	96.53	44.99	3.5	18	0.487	266	70.13	70.18		multiple vertical cracks
209-021-SV1-0.54	A054	96.98	44.97	3.5	20	0.464	255	69.20	69.32		multiple vertical cracks
209-021-SV1-0.89	A089	115.77	45.00	3.5	75	0.433	267	75.00	75.15		fragments, conical top and bottom ends
209-021-SV1-1.79	A179	100.13	45.11	3.5	75	0.459	269	70.65	70.85	70	2 fragments, curved plane
209-021-SV1-1.24	A124	109.63	45.00	3.5	125	0.440	246	69.86	69.64	65	3 fragments, curved plane, bottom wedge
209-030-DIL1-9.60	A960	102.44	44.94	3.5	125	0.440	239	67.58	67.23	67	3 fragments, shear plane, top wedge
209-021-SV1-0.66	A066	95.47	44.99	17.0	21	0.691	429	71.18	72.13	65	2 fragments, curved plane
209-021-SV1-0.76	A076	97.09	45.01	17.0	19	0.675	423	73.39	74.55	67	2 fragments, single shear plane
209-021-SV1-1.01	A101	117.16	45.02	17.0	75	0.695	423	71.37	72.56	65	2 fragments, curved plane
209-030-DIL1-8.30	A830	104.67	44.94	17.0	75	0.639	379	67.68	68.70	60	3 fragments, top wedge
209-021-SV1-1.35	A135	107.38	45.00	17.0	125	0.666	402	71.03	72.17	70	2 fragments, single shear plane
209-030-DIL1-9.70	A970	105.46	44.98	17.0	125	0.606	379	69.87	70.18	60	4 fragments, top and bottom wedges
209-021-SV1-1.58	A158	98.94	45.05	35.0	22	0.851	543	71.75	73.32	68	2 fragments, curved plane
209-021-SV1-1.69	A169	96.32	45.10	35.0	22	0.902	560	69.73	71.27		vertical cracks, bottom wedge
209-021-SV1-1.13	A113	106.87	45.02	35.0	75	0.880	538	69.15	70.61		2 fragments, top wedge
209-030-DIL1-8.60	A860	98.58	44.86	35.0	75	0.790	488	69.64	71.03	68	2 fragments, single shear plane
209-021-SV1-1.47	A147	111.74	45.03	35.0	125	0.829	518	69.64	71.08	64	3 fragments, curved plane, bottom wedge
209-030-DIL1-9.90	A990	102.36	44.98	35.0	125	0.806	496	68.39	69.75	68	2 fragments, 2 parallel shear planes

Table 3. Tangent Young's moduli of the rock samples

Specimen Identification	Pressure (MPa)	Temp. (deg C.)	Tangent Young's Modulus (GPa)									
			0.1	0.2	0.3	0.4	0.5	0.6	0.7	0.8	0.9	1.0
209-021-SV1-0.44	3.5	18	54.24	63.82	67.89	69.92	70.13	68.55	65.01	59.02	47.93	6.43
209-021-SV1-0.54	3.5	20	54.45	63.68	67.38	69.16	69.20	67.52	63.92	57.94	46.92	12.36
209-021-SV1-0.89	3.5	75	62.38	70.48	73.58	75.05	75.00	73.44	70.24	65.05	54.55	9.65
209-021-SV1-1.79	3.5	75	59.13	66.74	69.54	70.81	70.65	69.06	65.89	60.82	51.05	14.26
209-021-SV1-1.24	3.5	125	53.67	62.44	66.75	69.14	69.86	68.99	66.42	61.89	51.44	0.00
209-030-DIL1-9.60	3.5	125	50.44	58.89	63.81	66.59	67.58	66.87	64.40	59.87	49.39	4.83
209-021-SV1-0.66	17.0	21	71.85	73.90	73.84	72.95	71.18	68.45	64.60	59.34	50.94	16.30
209-021-SV1-0.76	17.0	19	74.35	76.82	76.66	75.54	73.39	70.09	65.42	58.93	49.04	18.88
209-021-SV1-1.01	17.0	75	73.82	75.19	74.85	73.60	71.37	68.02	63.34	56.89	46.98	12.77
209-030-DIL1-8.30	17.0	75	70.15	71.01	70.68	69.59	67.68	64.86	60.96	55.70	48.10	15.25
209-021-SV1-1.35	17.0	125	73.47	74.12	74.13	73.12	71.03	67.72	62.94	56.21	46.29	12.06
209-030-DIL1-9.70	17.0	125	78.21	72.75	70.03	70.22	69.87	67.81	63.82	57.35	47.06	25.97
209-021-SV1-1.58	35.0	22	78.57	79.16	77.25	74.80	71.75	67.98	63.34	57.57	48.84	25.50
209-021-SV1-1.69	35.0	22	78.26	77.30	75.23	72.73	69.73	66.16	61.87	56.68	49.43	16.73
209-021-SV1-1.13	35.0	75	76.50	75.89	74.21	71.99	69.15	65.58	61.14	55.54	47.44	18.98
209-030-DIL1-8.60	35.0	75	76.83	75.94	74.41	72.33	69.64	66.23	61.95	56.56	49.05	17.57
209-021-SV1-1.47	35.0	125	77.06	76.17	74.57	72.42	69.64	66.14	61.76	56.23	48.84	19.46
209-030-DIL1-9.90	35.0	125	75.13	74.27	72.95	71.02	68.39	64.96	60.55	54.86	47.08	24.45

Table 4. Pseudo Young's moduli of the rock samples

Specimen Identification	Pressure (MPa)	Temp. (deg C.)	Pseudo Young's Modulus (GPa)									
			0.1	0.2	0.3	0.4	0.5	0.6	0.7	0.8	0.9	1.0
209-021-SV1-0.44	3.5	18	38.34	59.93	66.02	69.06	70.18	69.50	66.94	62.20	54.09	29.46
209-021-SV1-0.54	3.5	20	40.34	59.94	65.69	68.42	69.32	68.51	65.88	61.11	52.97	30.77
209-021-SV1-0.89	3.5	75	49.67	67.35	72.16	74.44	75.15	74.35	71.98	67.80	60.62	34.58
209-021-SV1-1.79	3.5	75	46.23	63.85	68.26	70.29	70.85	69.98	67.60	63.50	56.64	34.56
209-021-SV1-1.24	3.5	125	44.32	58.62	64.75	68.09	69.64	69.56	67.84	64.31	57.53	29.22
209-030-DIL1-9.60	3.5	125	43.28	54.99	61.52	65.35	67.23	67.36	65.78	62.30	55.41	29.81
209-021-SV1-0.66	17.0	21	64.60	73.41	73.94	73.46	72.13	69.89	66.61	62.06	55.65	35.70
209-021-SV1-0.76	17.0	19	65.15	76.26	76.82	76.18	74.55	71.83	67.86	62.30	54.38	34.92
209-021-SV1-1.01	17.0	75	69.81	74.87	75.10	74.30	72.56	69.78	65.78	60.23	52.35	31.47
209-030-DIL1-8.30	17.0	75	63.96	70.83	70.91	70.20	68.70	66.34	62.99	58.42	52.18	34.33
209-021-SV1-1.35	17.0	125	74.17	73.74	74.21	73.72	72.17	69.47	65.44	59.71	51.49	31.30
209-030-DIL1-9.70	17.0	125	81.37	75.25	71.13	69.95	70.18	68.98	65.97	60.77	52.46	36.06
209-021-SV1-1.58	35.0	22	74.38	79.46	78.24	76.07	73.32	69.91	65.72	60.52	53.63	37.23
209-021-SV1-1.69	35.0	22	74.70	78.08	76.29	74.01	71.27	67.98	64.06	59.33	53.42	35.00
209-021-SV1-1.13	35.0	75	74.46	76.44	75.09	73.14	70.61	67.42	63.42	58.40	51.87	34.19
209-030-DIL1-8.60	35.0	75	75.97	76.47	75.21	73.41	71.03	67.98	64.14	59.32	53.10	34.52
209-021-SV1-1.47	35.0	125	74.42	76.74	75.41	73.54	71.08	67.94	64.01	59.06	52.72	36.05
209-030-DIL1-9.90	35.0	125	76.43	74.69	73.66	72.03	69.75	66.73	62.82	57.78	51.17	36.72

Table 5. Values of σ_c , m , s and r^2 computed by using the Hoek and Brown failure criterion.

Test Temperature (°C.)	Number of Samples n	Estimated Uniaxial Compressive Strength σ_c (MPa)	m	s	r^2
22	3	246	28.28	1.00	0.9835
75	6	231	26.31	1.00	0.9483
125	6	200	31.27	1.00	0.9870

Table 6. Strength properties of rock samples.

Test Temperature (°C)	Confining Pressure (MPa)	Angle of Internal Friction (degree)	Cohesion (MPa)
22	17.0	55	43
22	35.0	48	66
75	3.5	58	36
75	17.0	54	43
75	35.0	47	66
125	3.5	59	30
125	17.0	55	39
125	35.0	48	62

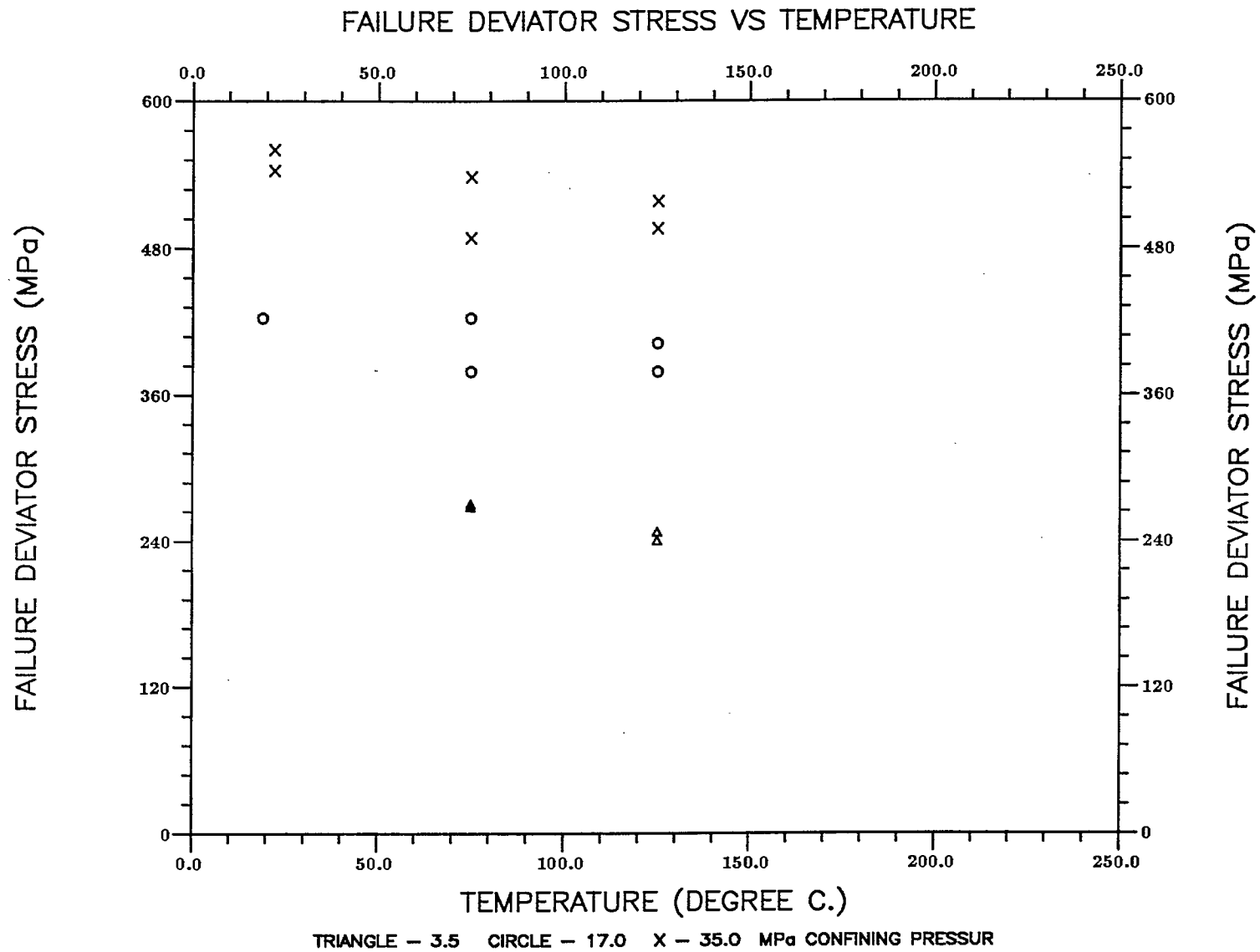


Figure 1. Plots of failure deviator stresses versus temperature for tests conducted at the confining pressures of 3.5, 17.0 and 35.0 MPa.

TANGENT YOUNG'S MODULUS VS NORMALIZED DEVIATOR STRESS (18 - 22 DEG. C.)

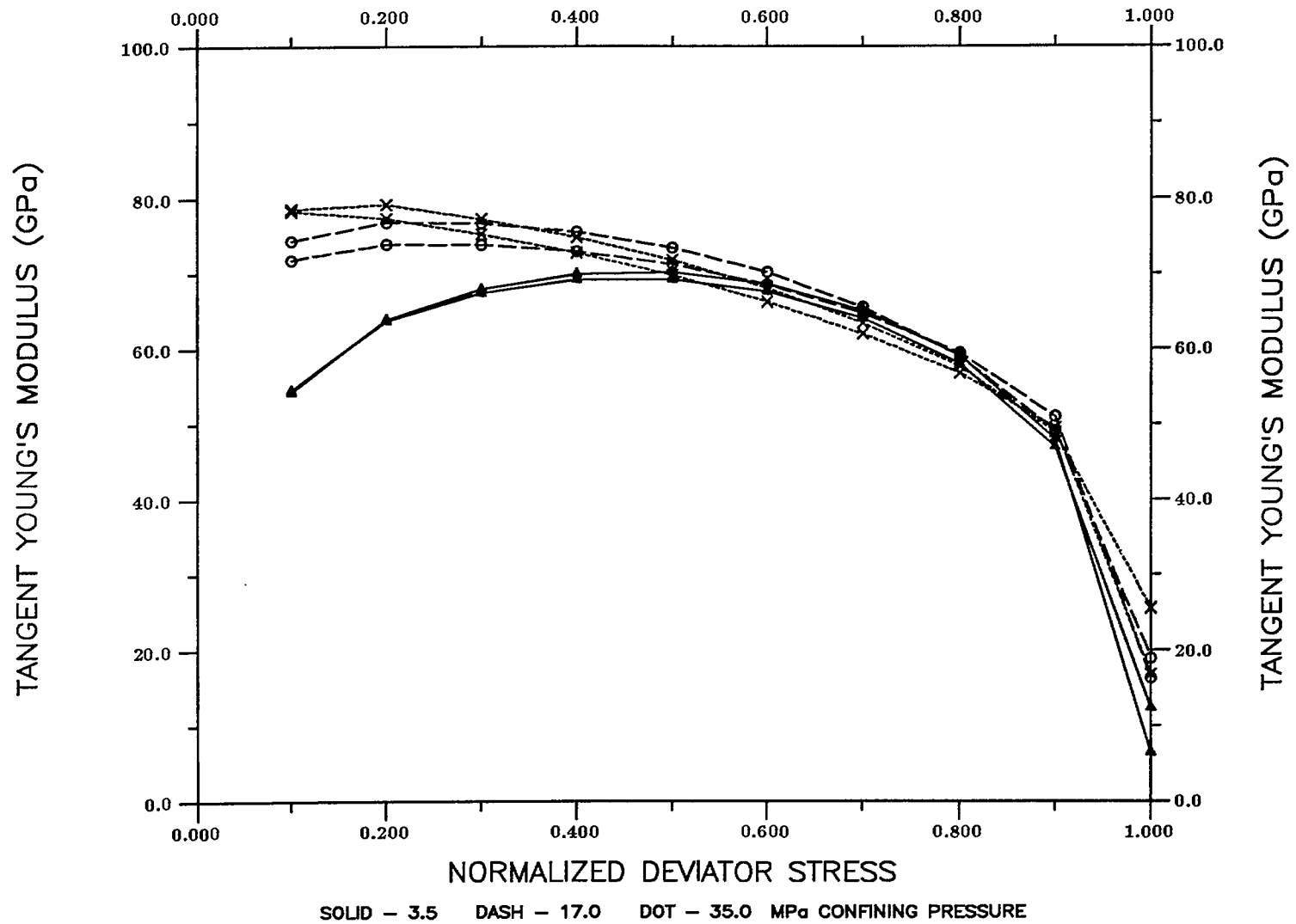


Figure 2. Plots of tangent Young's modulus versus normalized deviator stress for tests conducted at the ambient temperature.

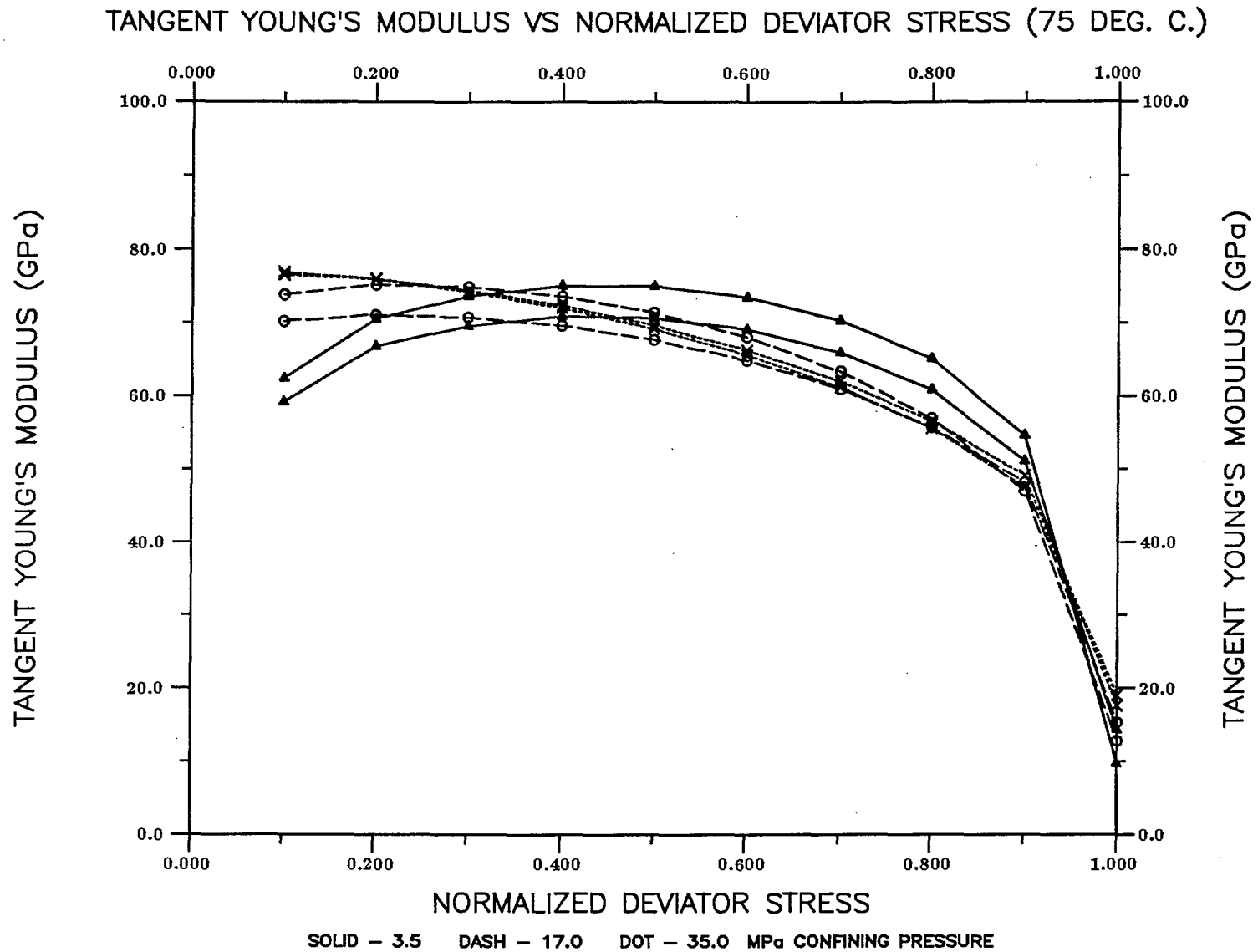


Figure 3. Plots of tangent Young's modulus versus normalized deviator stress for tests conducted at the temperature of 75° C.

TANGENT YOUNG'S MODULUS VS NORMALIZED DEVIATOR STRESS (125 DEG. C.)

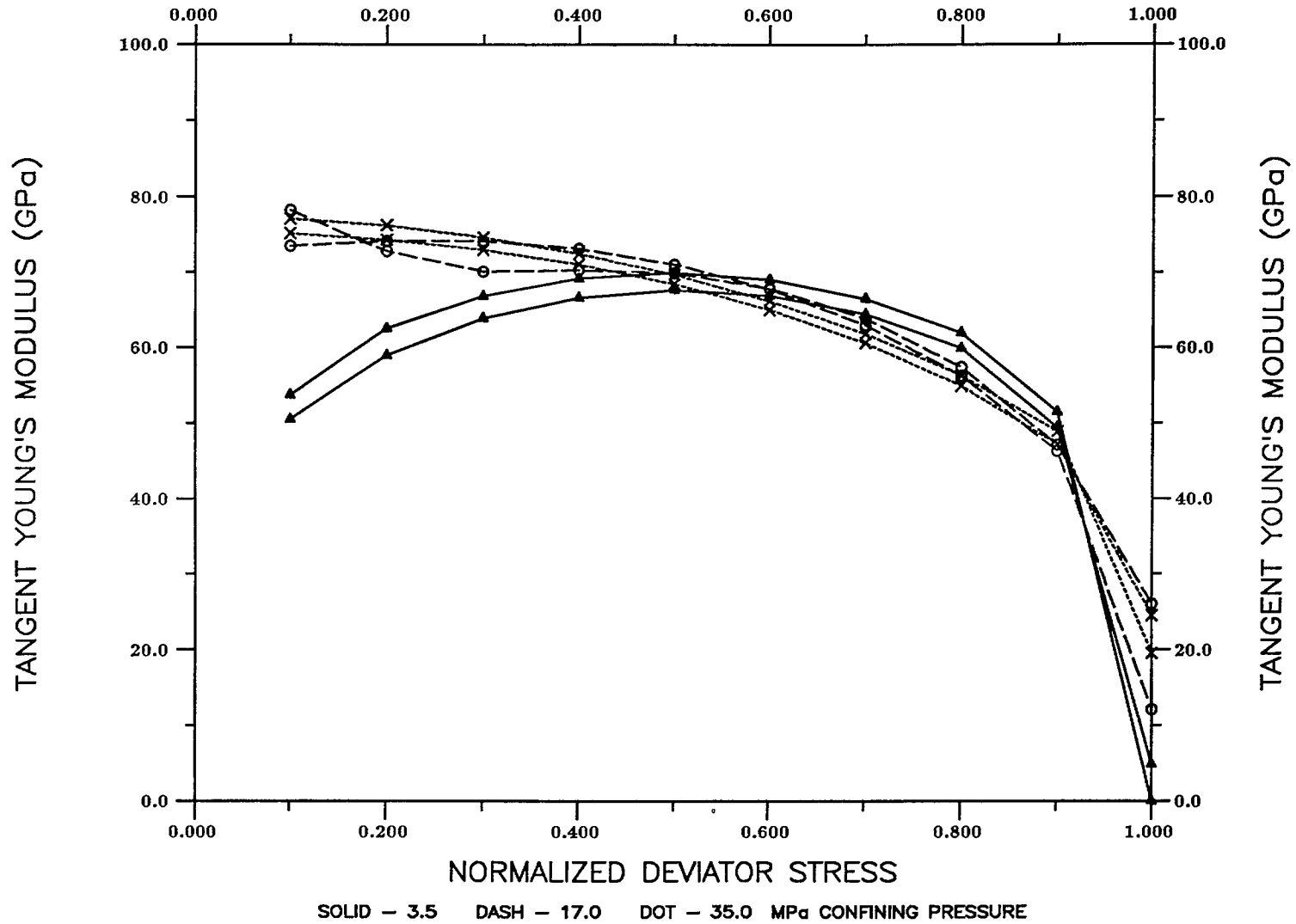


Figure 4. Plots of tangent Young's modulus versus normalized deviator stress for tests conducted at the temperature of 125° C.

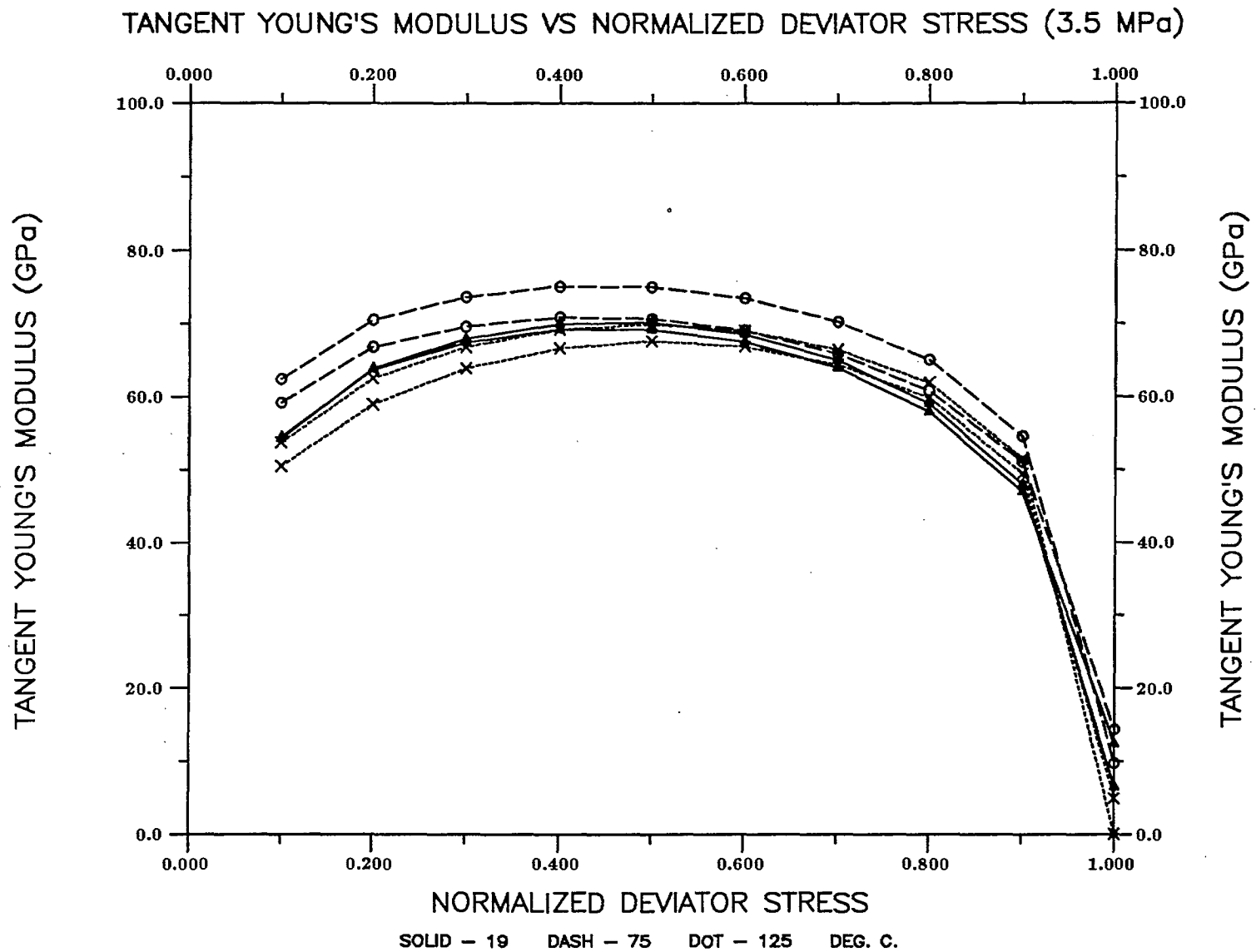


Figure 5. Plots of tangent Young's modulus versus normalized deviator stress for tests conducted at the confining pressure of 3.5 MPa.

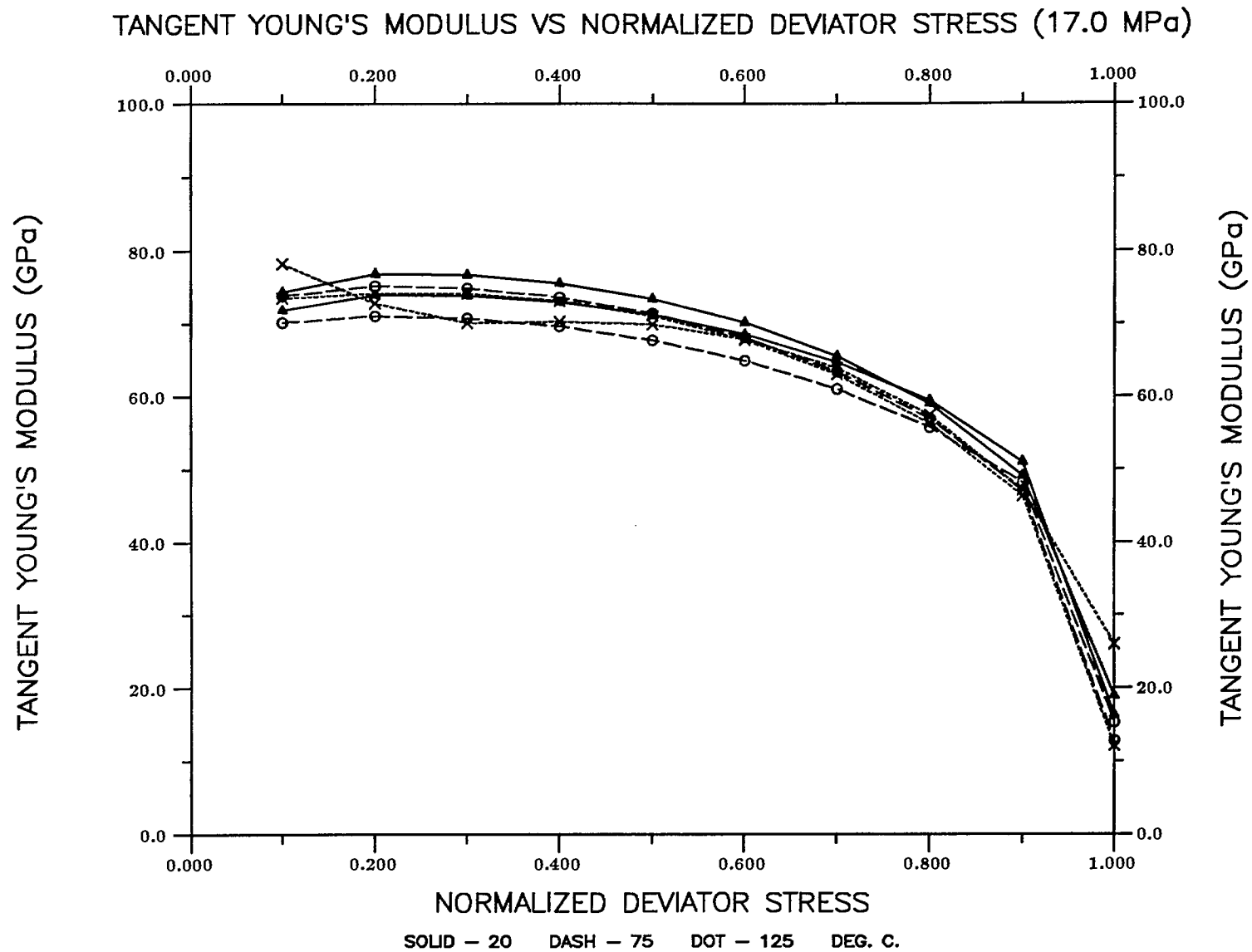


Figure 6. Plots of tangent Young's modulus versus normalized deviator stress for tests conducted at the confining pressure of 17.0 MPa.

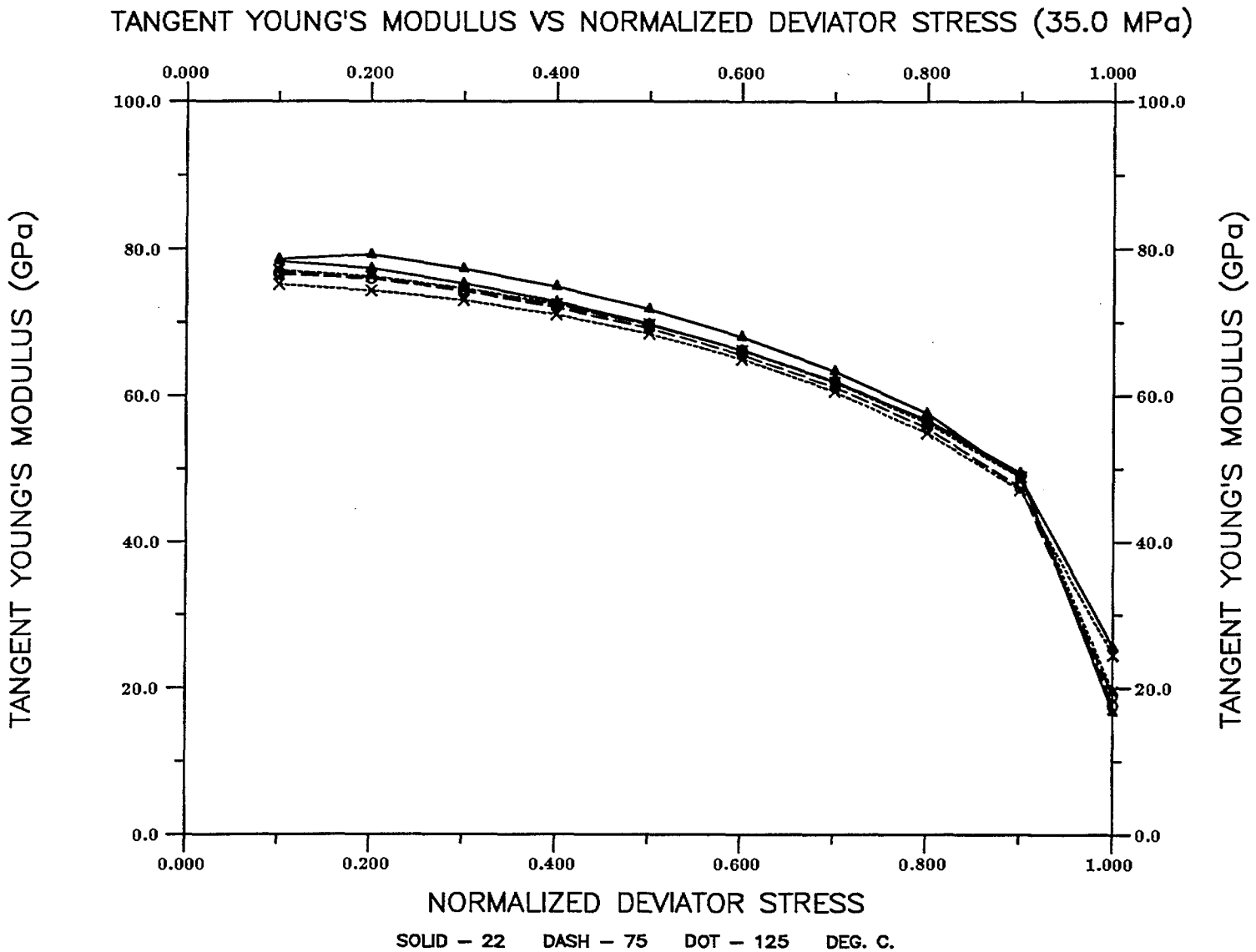


Figure 7. Plots of tangent Young's modulus versus normalized deviator stress for tests conducted at the confining pressure of 35.0 MPa.

PSEUDO YOUNG'S MODULUS VS NORMALIZED DEVIATOR STRESS (18 - 22 DEG. C.)

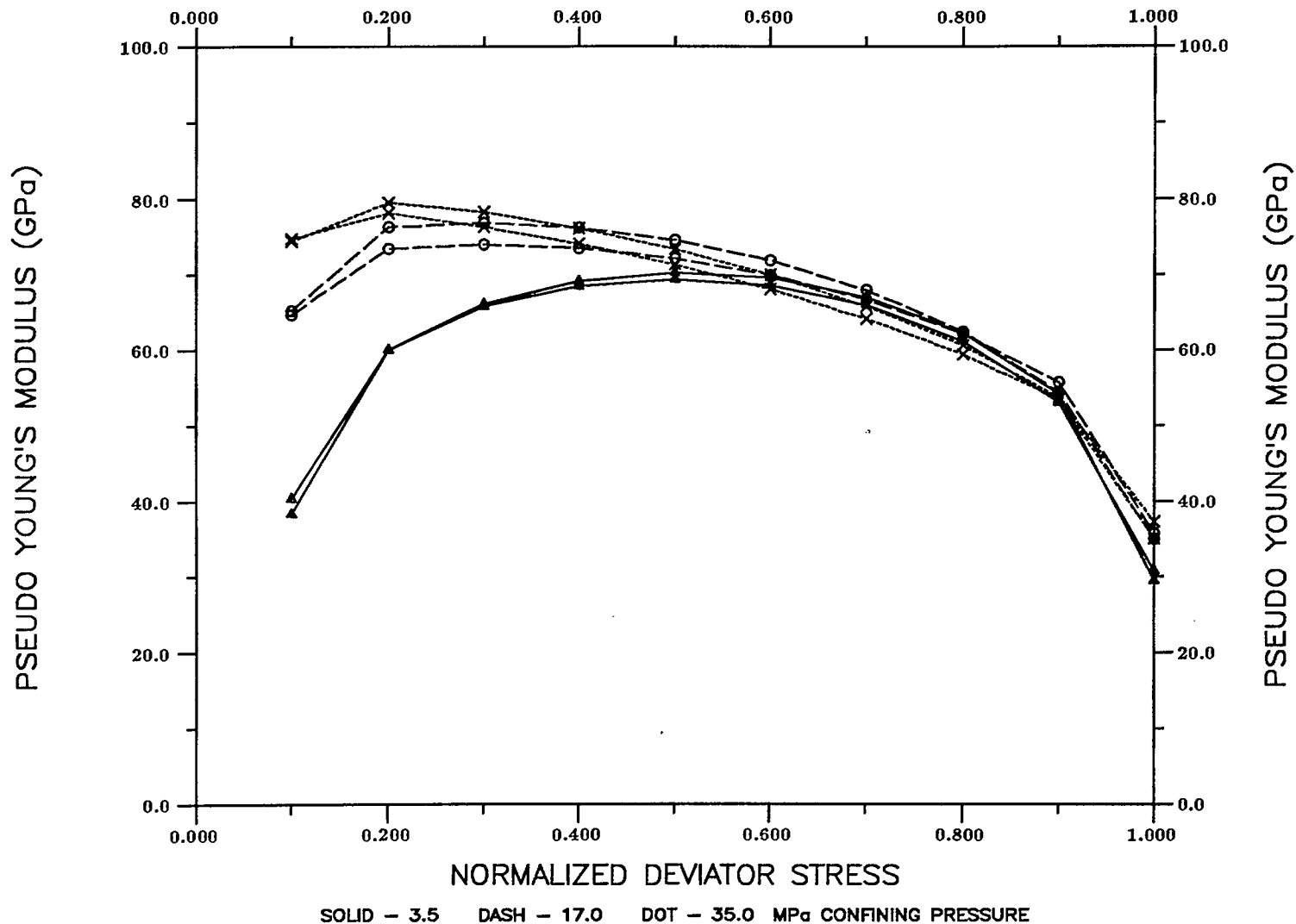


Figure 8. Plots of pseudo Young's modulus versus normalized deviator stress for tests conducted at the ambient temperature.

PSEUDO YOUNG'S MODULUS VS NORMALIZED DEVIATOR STRESS (75 DEG. C.)

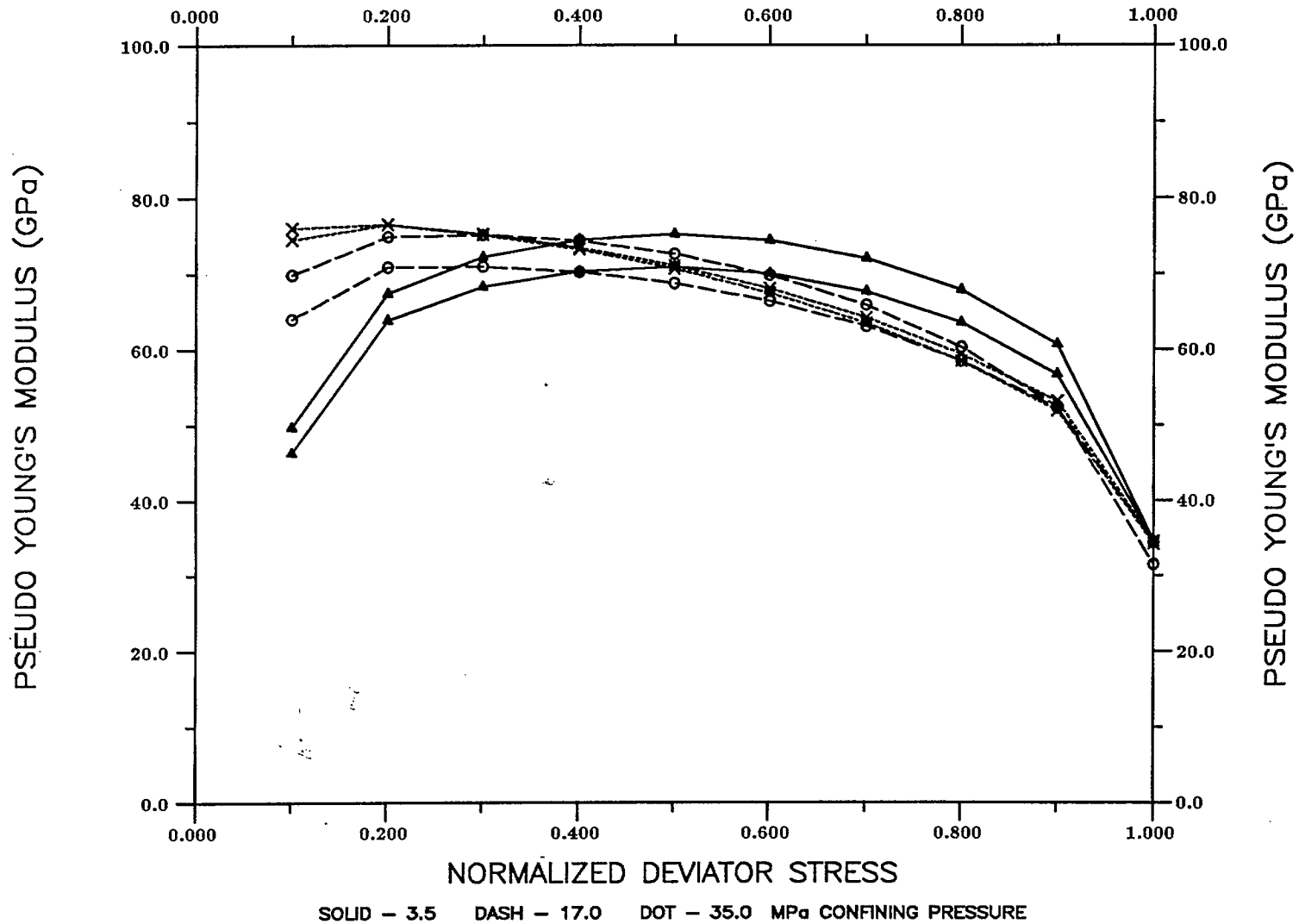


Figure 9. Plots of pseudo Young's modulus versus normalized deviator stress for tests conducted at the temperature of 75° C.

PSEUDO YOUNG'S MODULUS VS NORMALIZED DEVIATOR STRESS (125 DEG. C.)

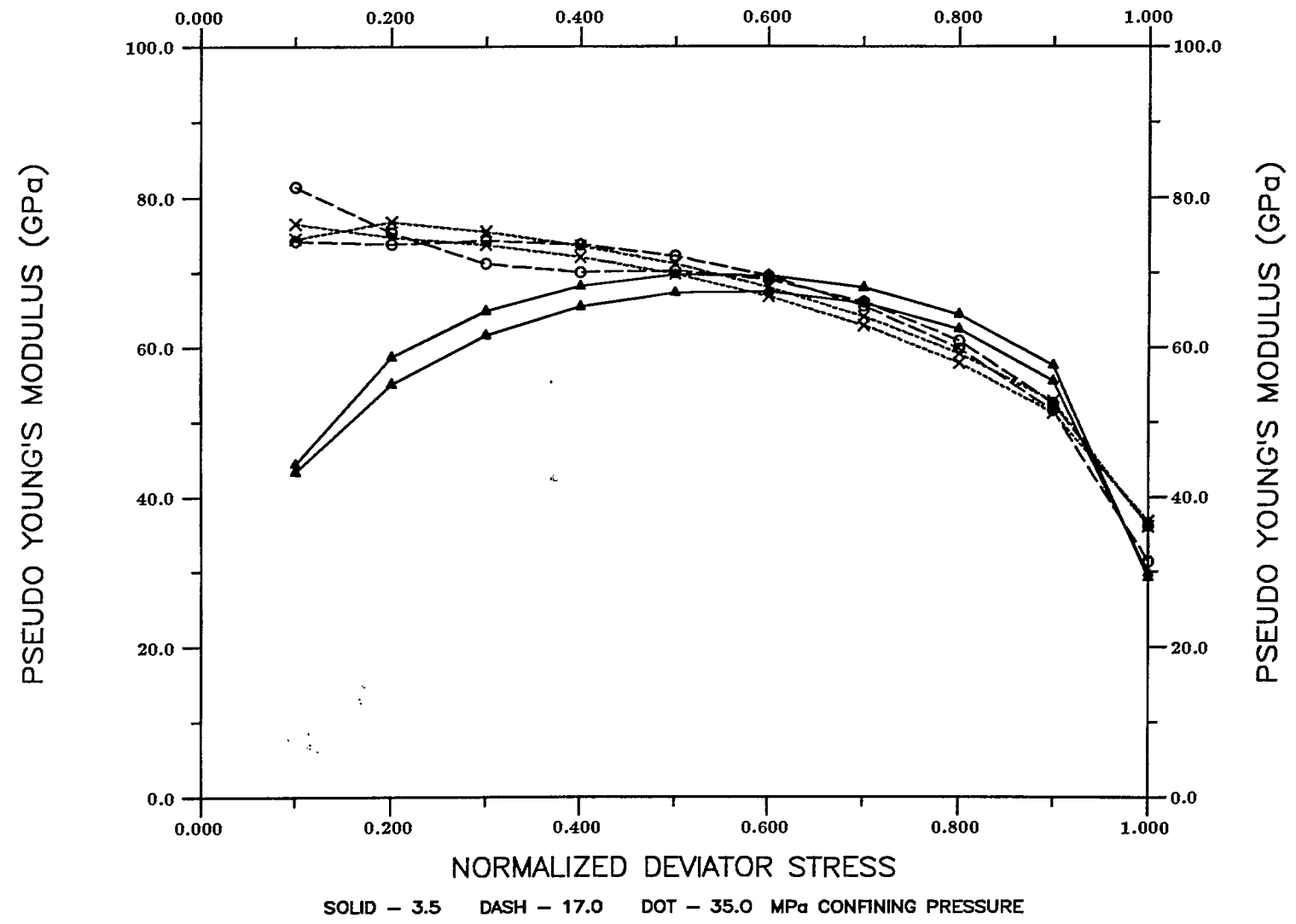


Figure 10. Plots of pseudo Young's modulus versus normalized deviator stress for tests conducted at the temperature of 125° C.

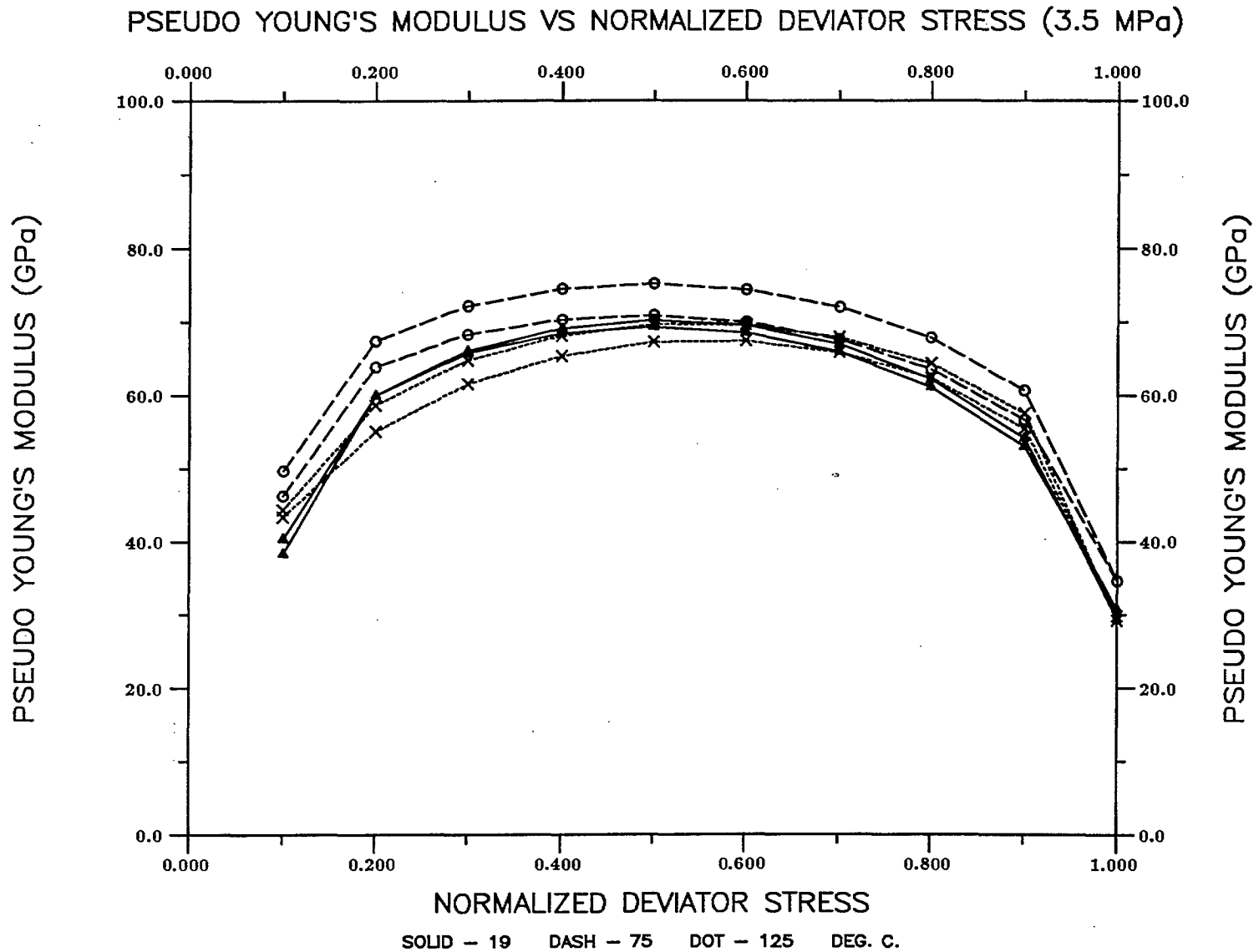


Figure 11. Plots of pseudo Young's modulus versus normalized deviator stress for tests conducted at the confining pressure of 3.5 MPa.

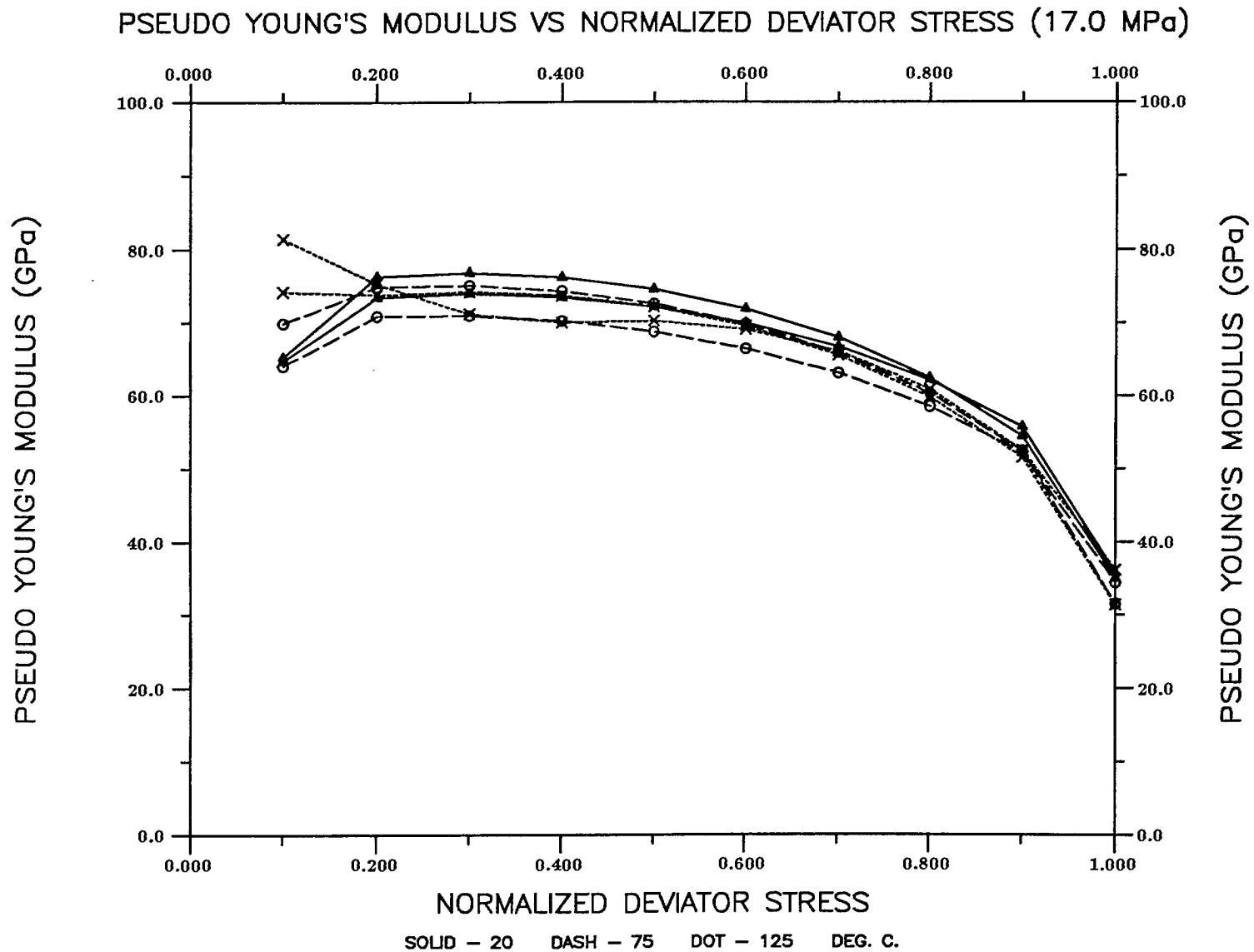


Figure 12. Plots of pseudo Young's modulus versus normalized deviator stress for tests conducted at the confining pressure of 17.0 MPa.

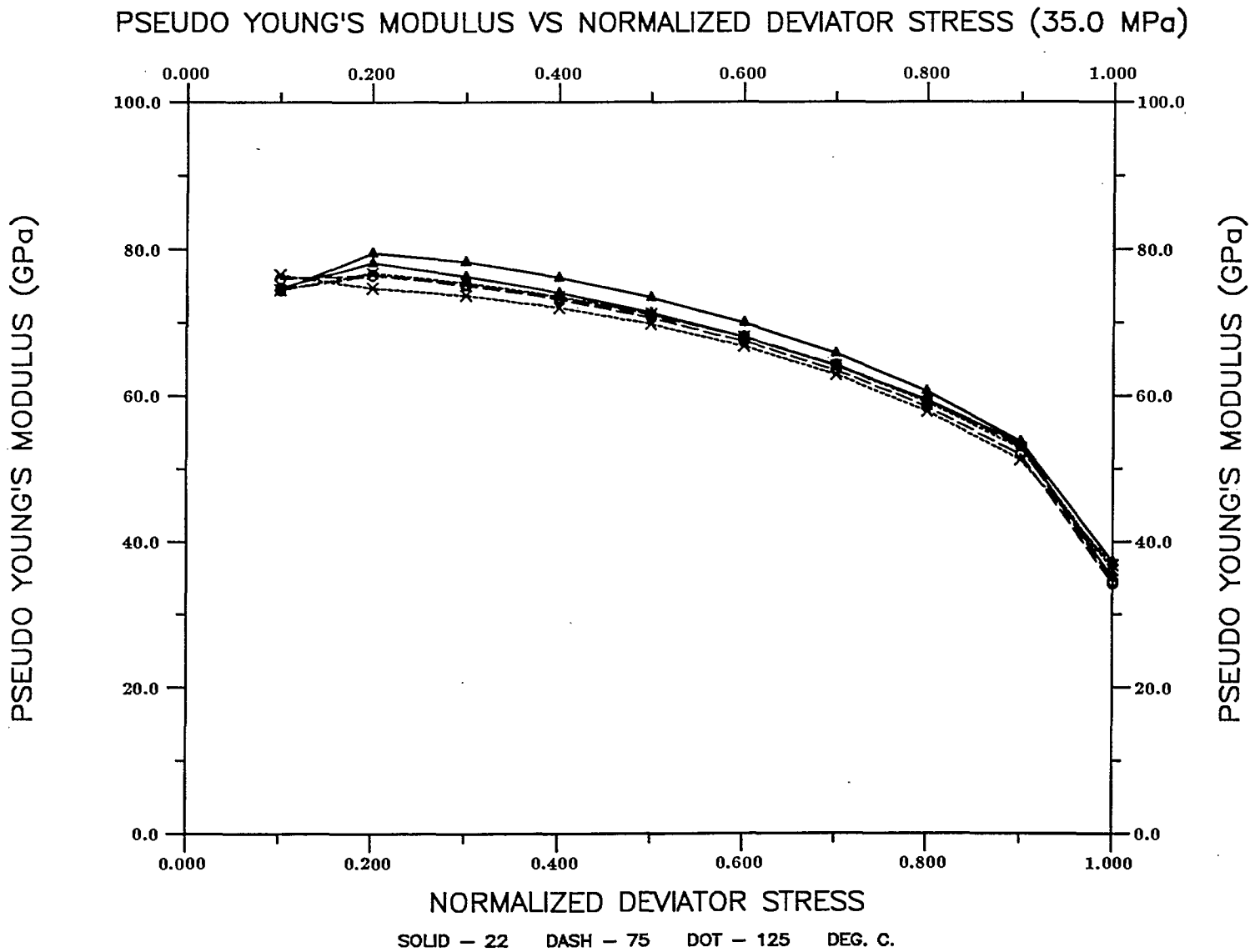
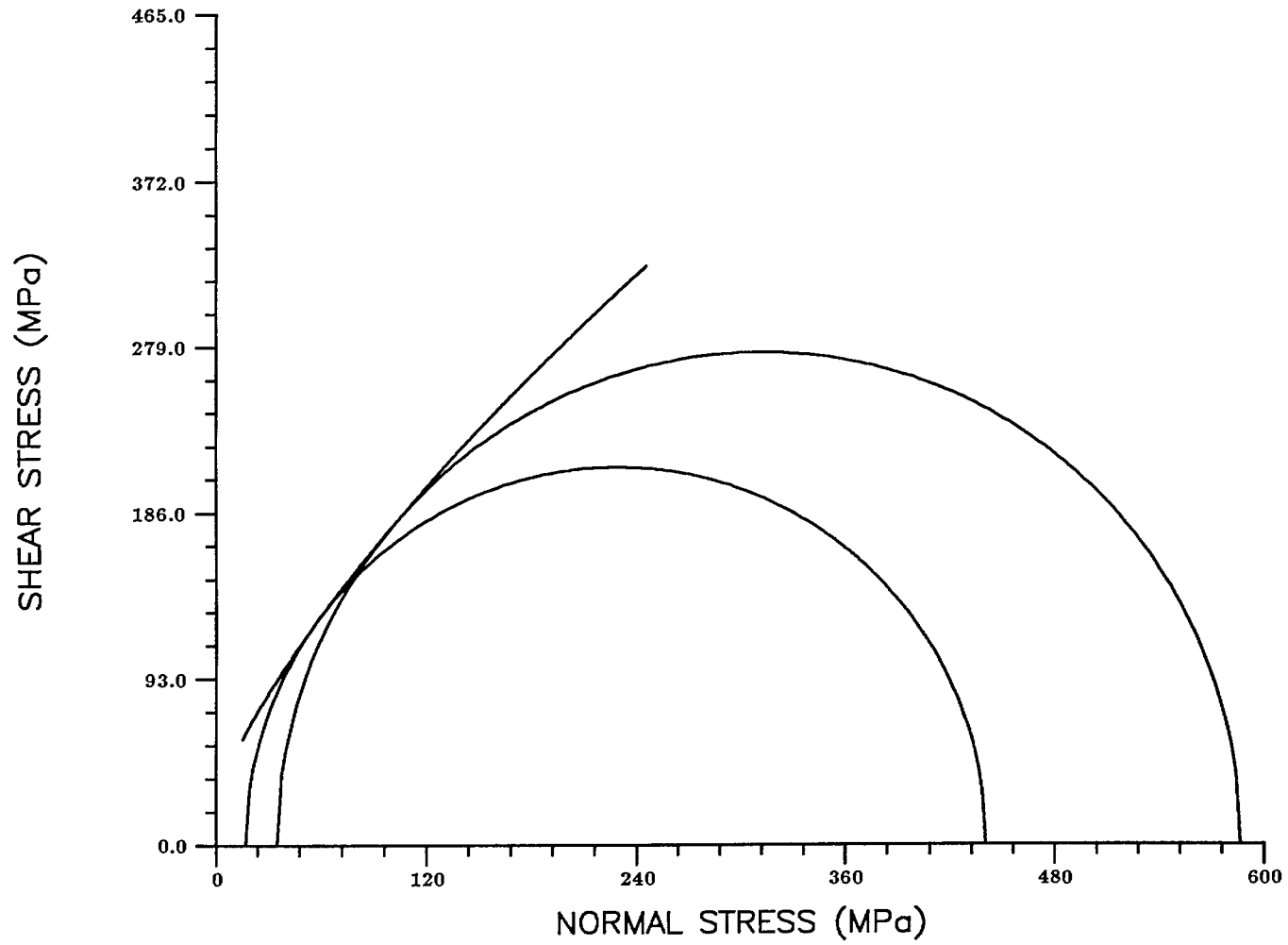


Figure 13. Plots of pseudo Young's modulus versus normalized deviator stress for tests conducted at the confining pressure of 35.0 MPa.

MOHR CIRCLES AND FAILURE ENVELOPE (19 - 22 DEG C.)



35

Figure 14. Mohr circles and failure envelope for tests carried out at the ambient temperature

MOHR CIRCLES AND FAILURE ENVELOPE (75 DEG C.)

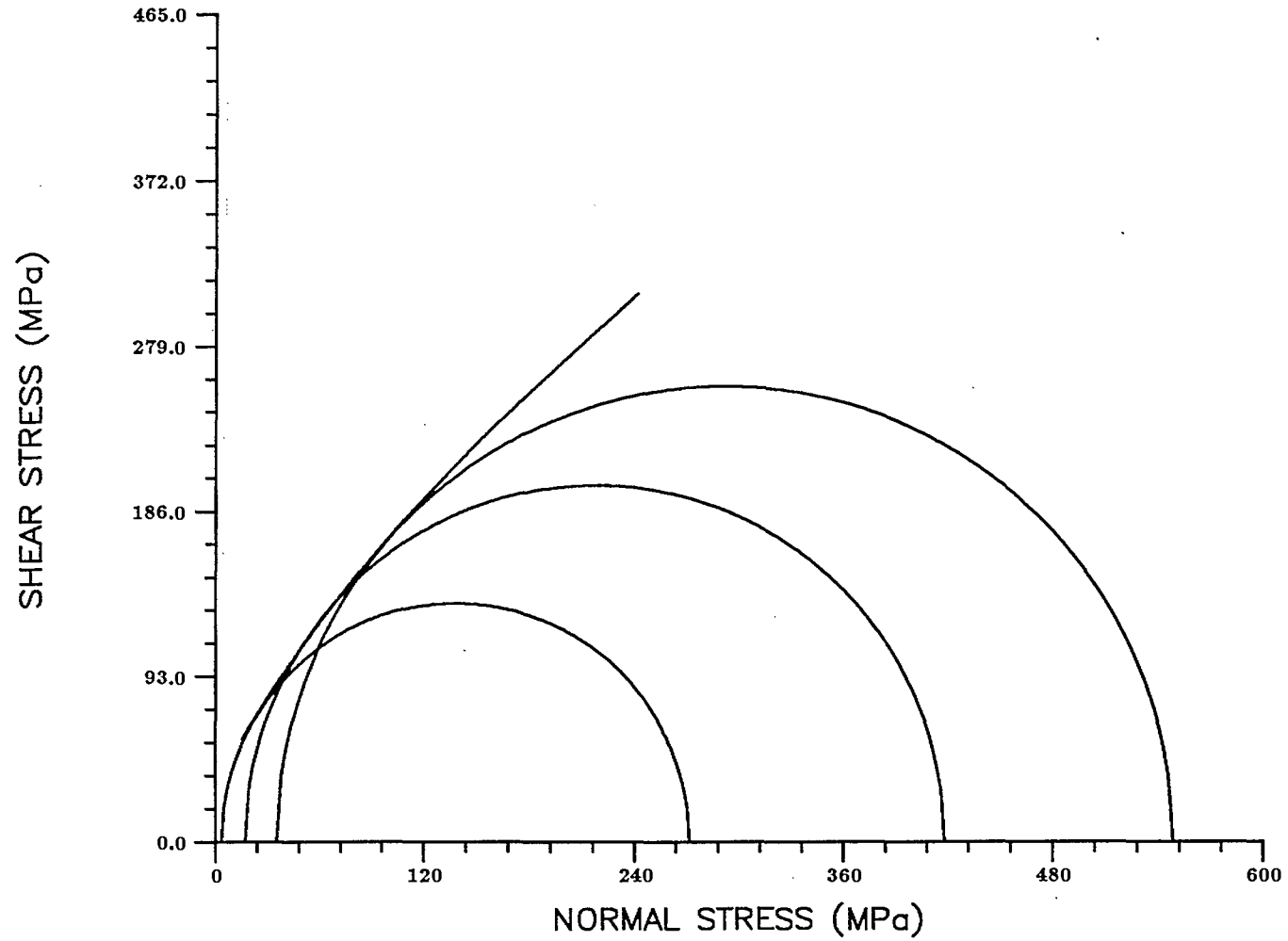


Figure 15. Mohr circles and failure envelope for tests carried out at the temperature of 75° C.

MOHR CIRCLES AND FAILURE ENVELOPE (125 DEG C.)

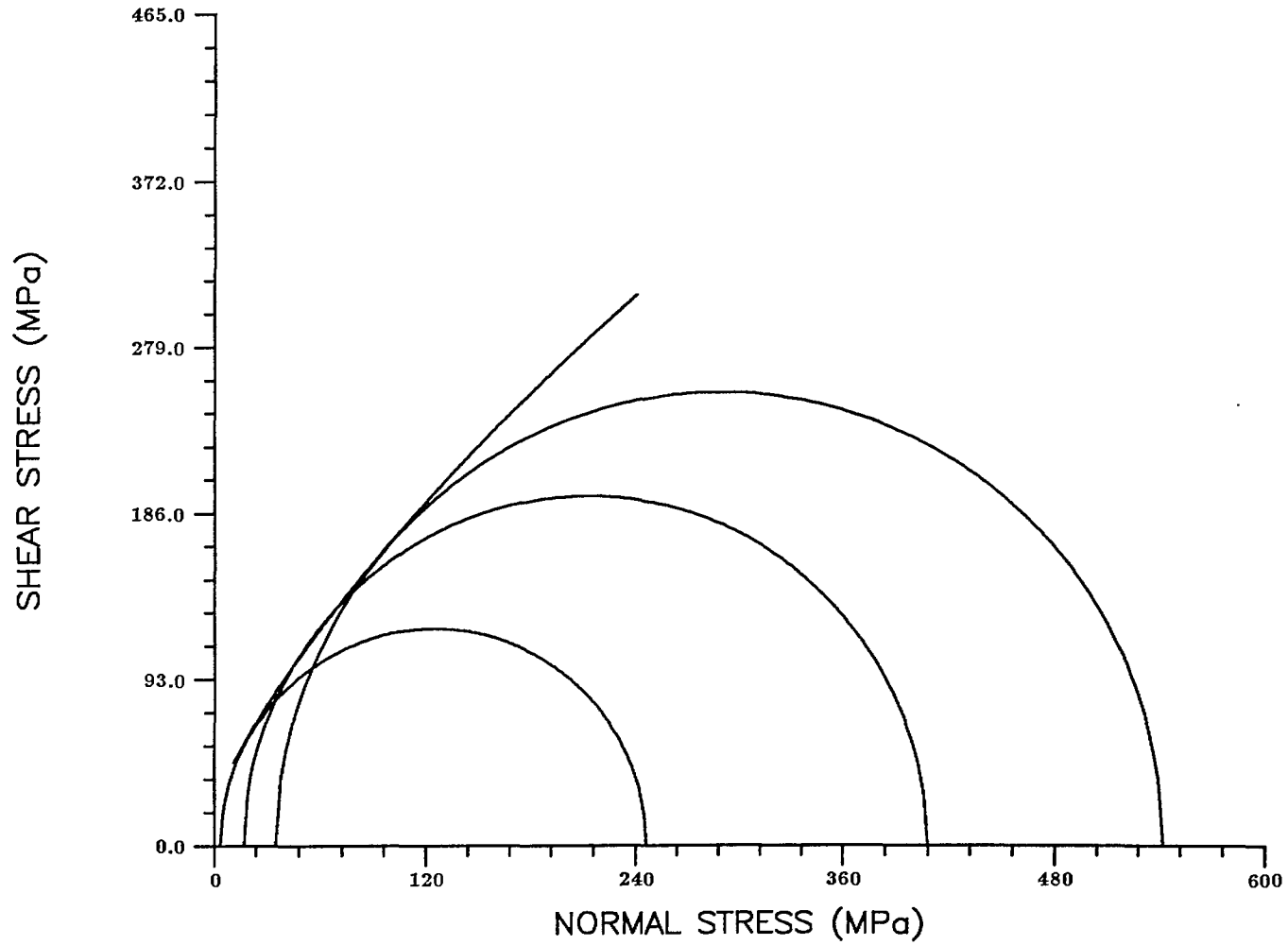


Figure 16. Mohr circles and failure envelope for tests carried out at the temperature of 125° C.

MOHR FAILURE ENVELOPES

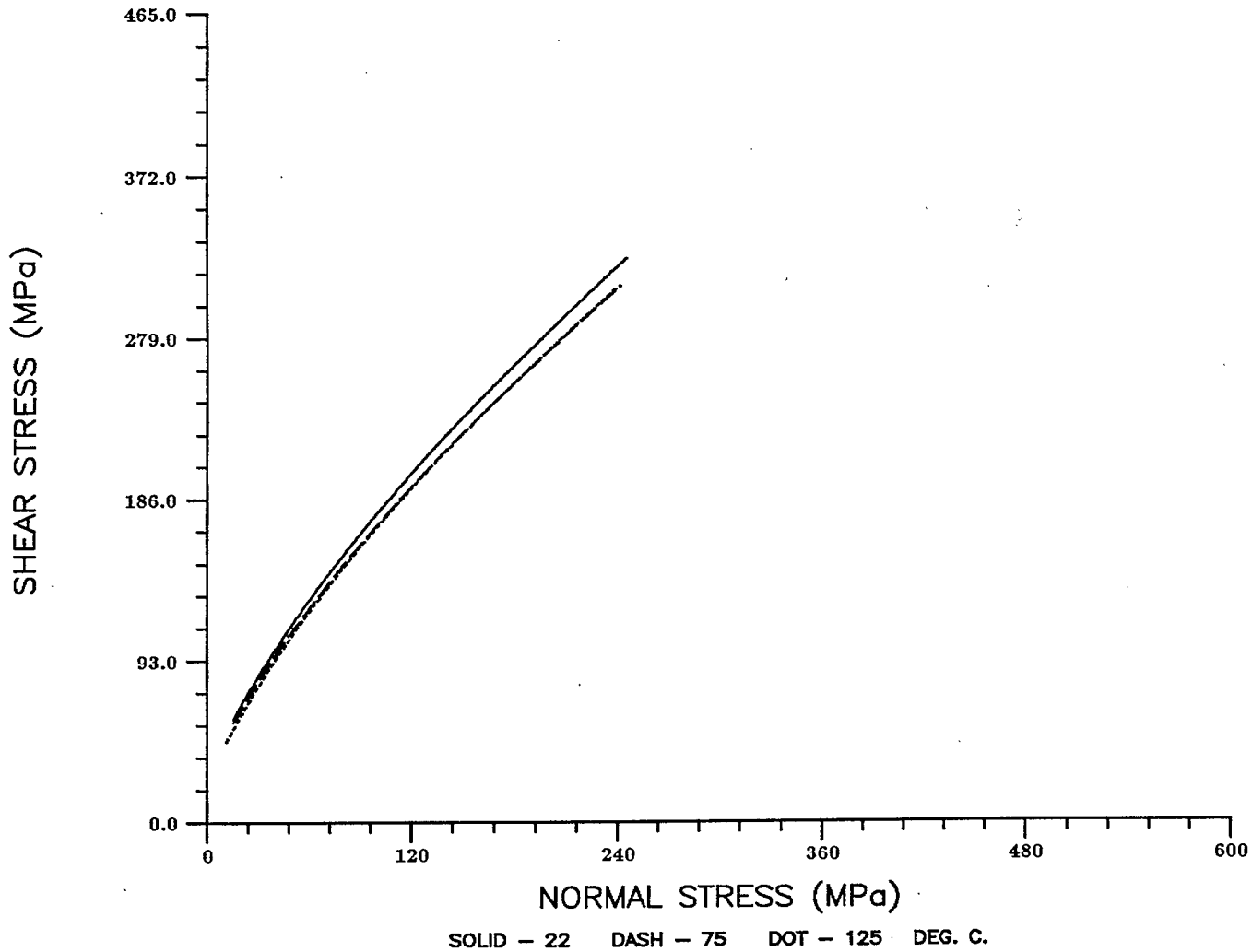


Figure 17. Failure envelopes for tests carried out at the temperatures of 22°, 75° and 100° C.

Appendix A

Stress-strain curves

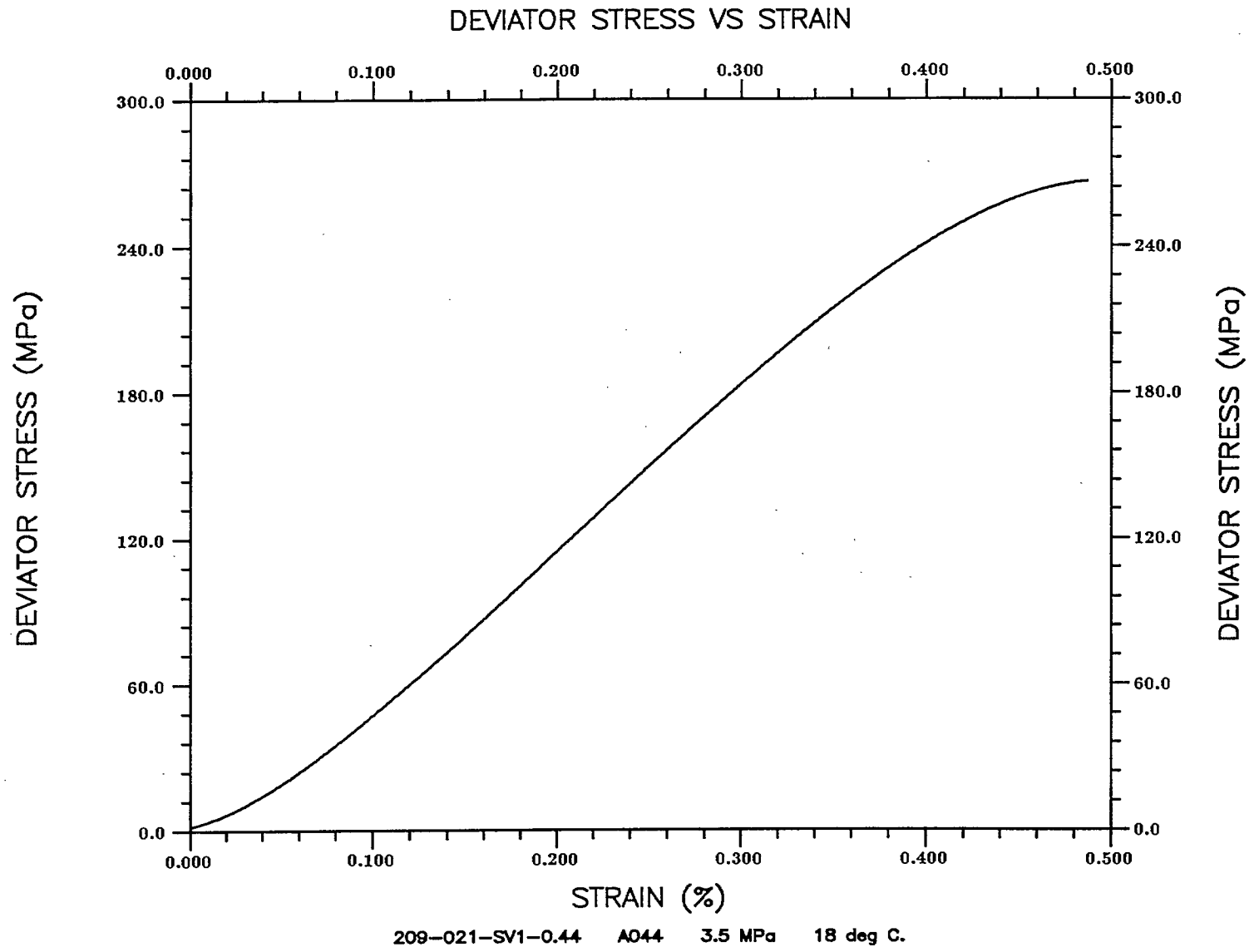


Figure A.1. Specimen 209-021-SV1-0.44 ($\sigma_3 = 3.5$ MPa, temperature = 18° C)

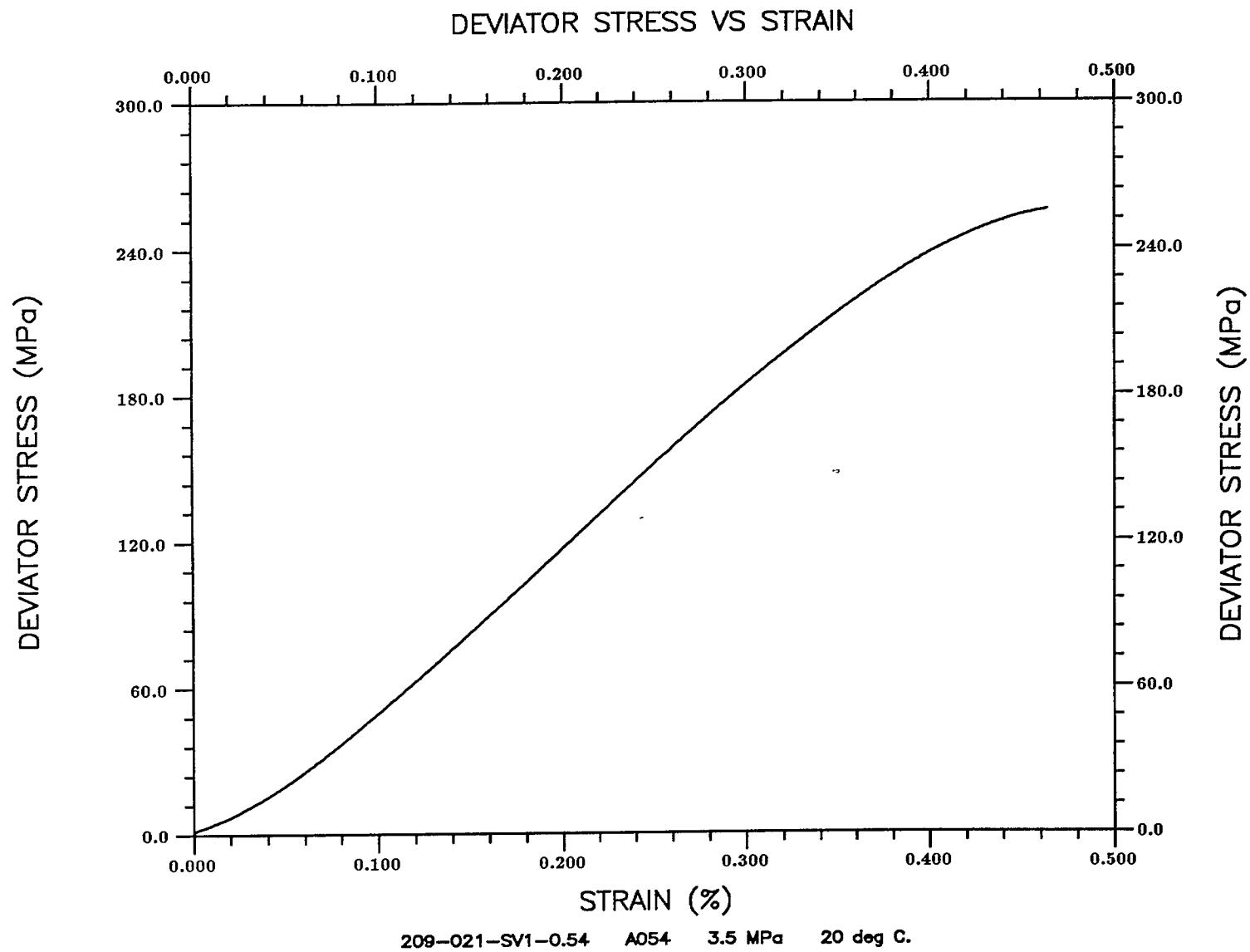


Figure A.2. Specimen 209-021-SV1-0.54 ($\sigma_3 = 3.5$ MPa, temperature = 20° C)

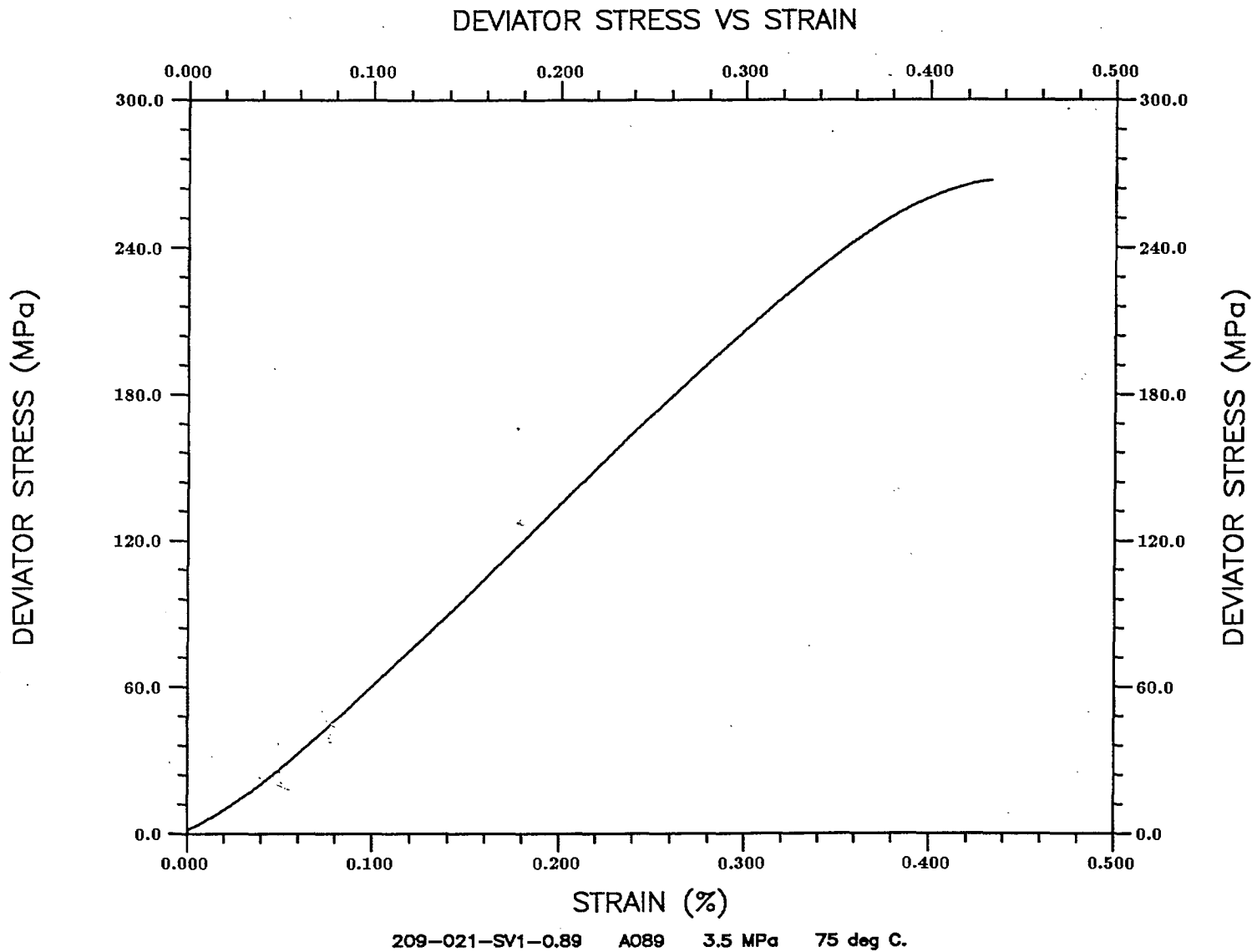


Figure A.3. Specimen 209-021-SV1-0.89 ($\sigma_3 = 3.5$ MPa, temperature = 75° C)

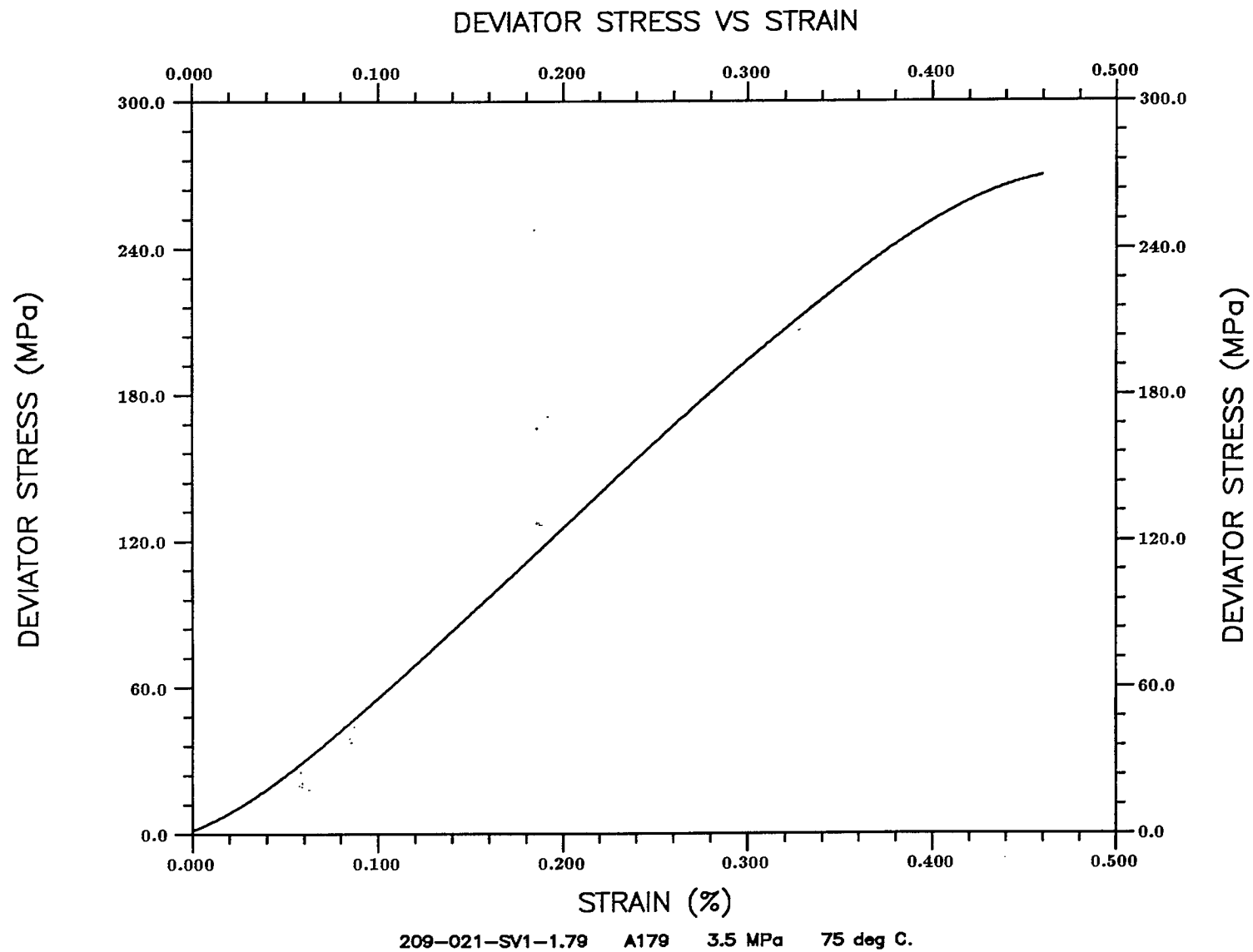


Figure A.4. Specimen 209-021-SV1-1.79 ($\sigma_3 = 3.5$ MPa, temperature = 75° C)

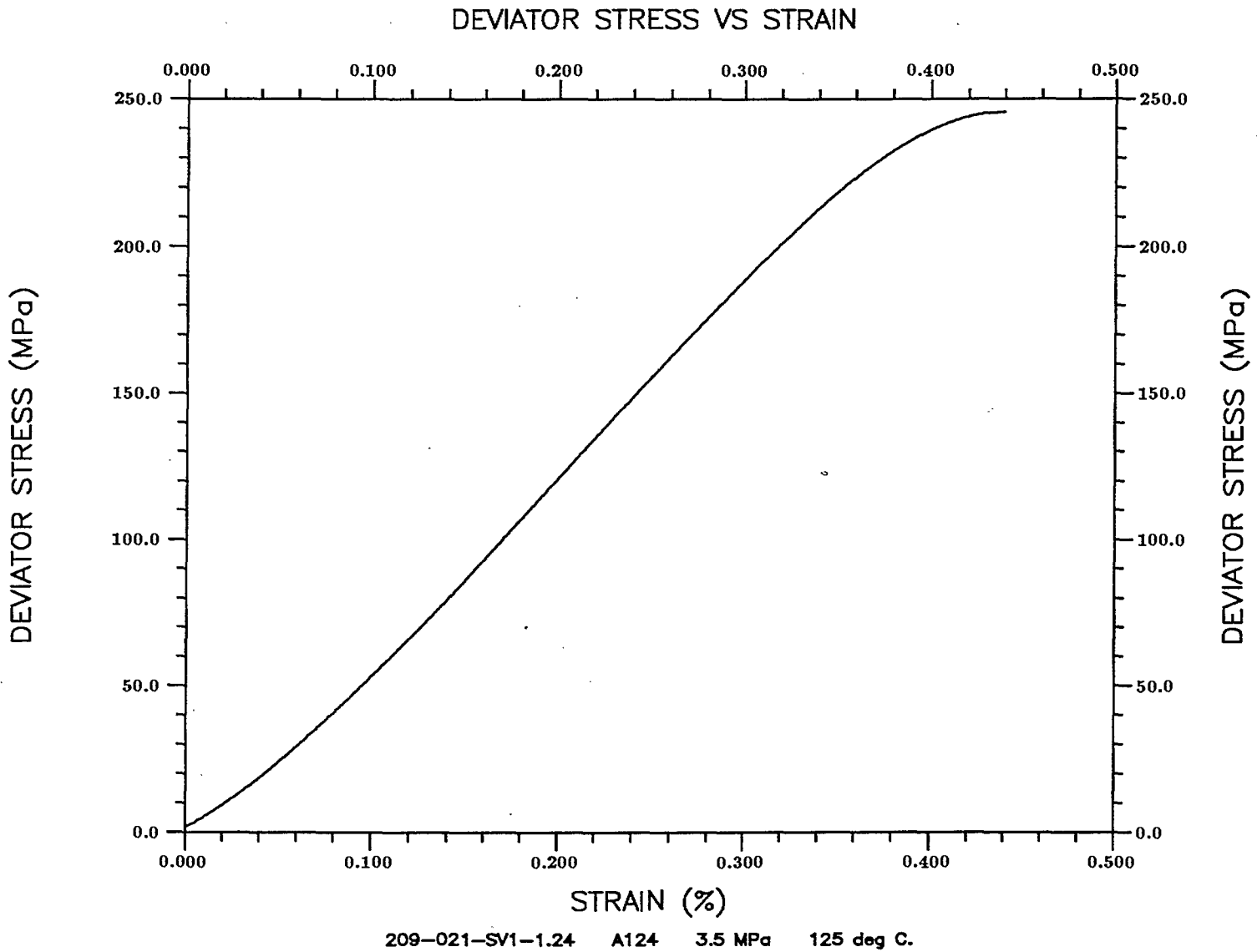


Figure A.5. Specimen 209-021-SV1-1.24 ($\sigma_3 = 3.5$ MPa, temperature = 125° C)

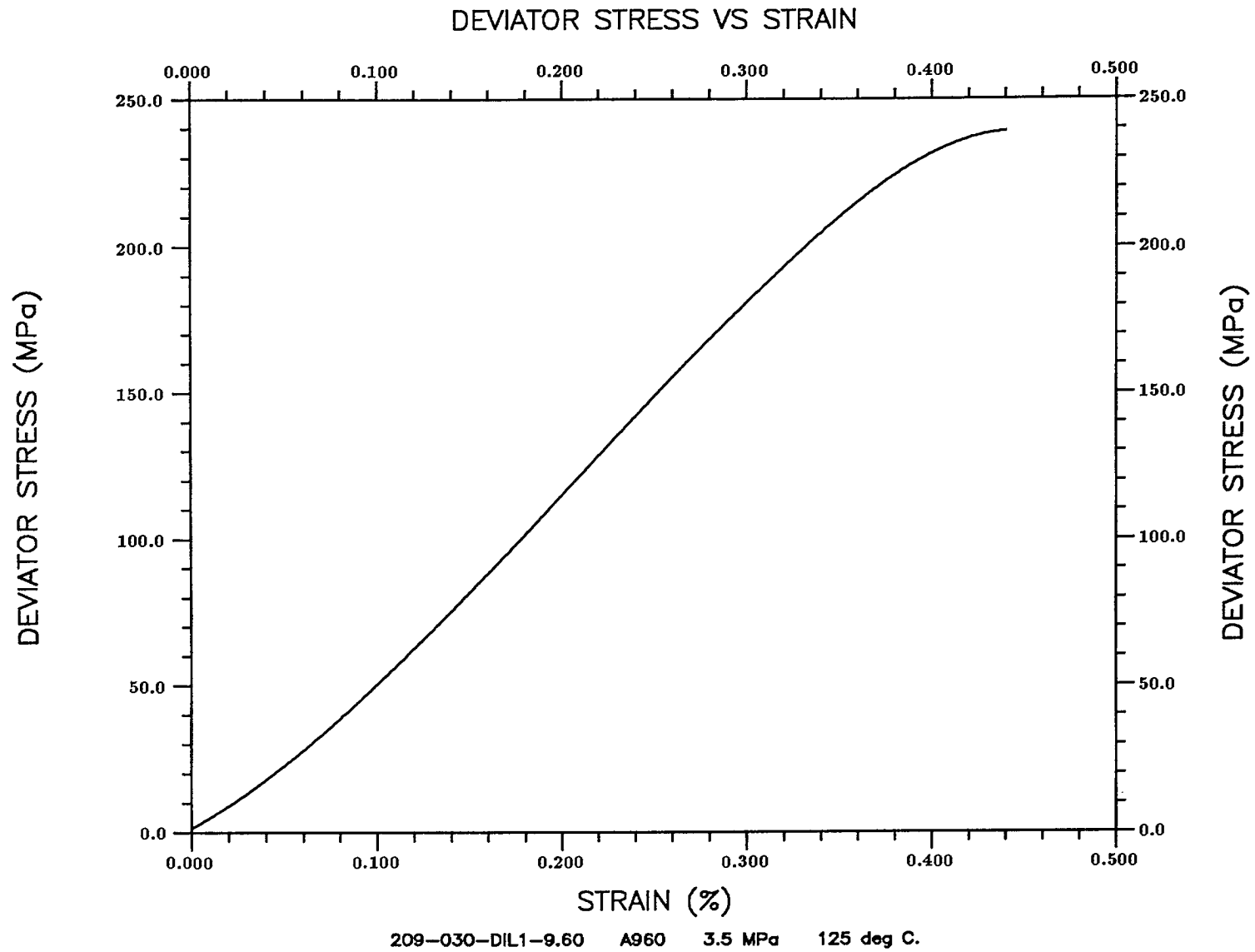


Figure A.6. Specimen 209-030-DIL1-9.60 ($\sigma_3 = 3.5$ MPa, temperature = 125° C)

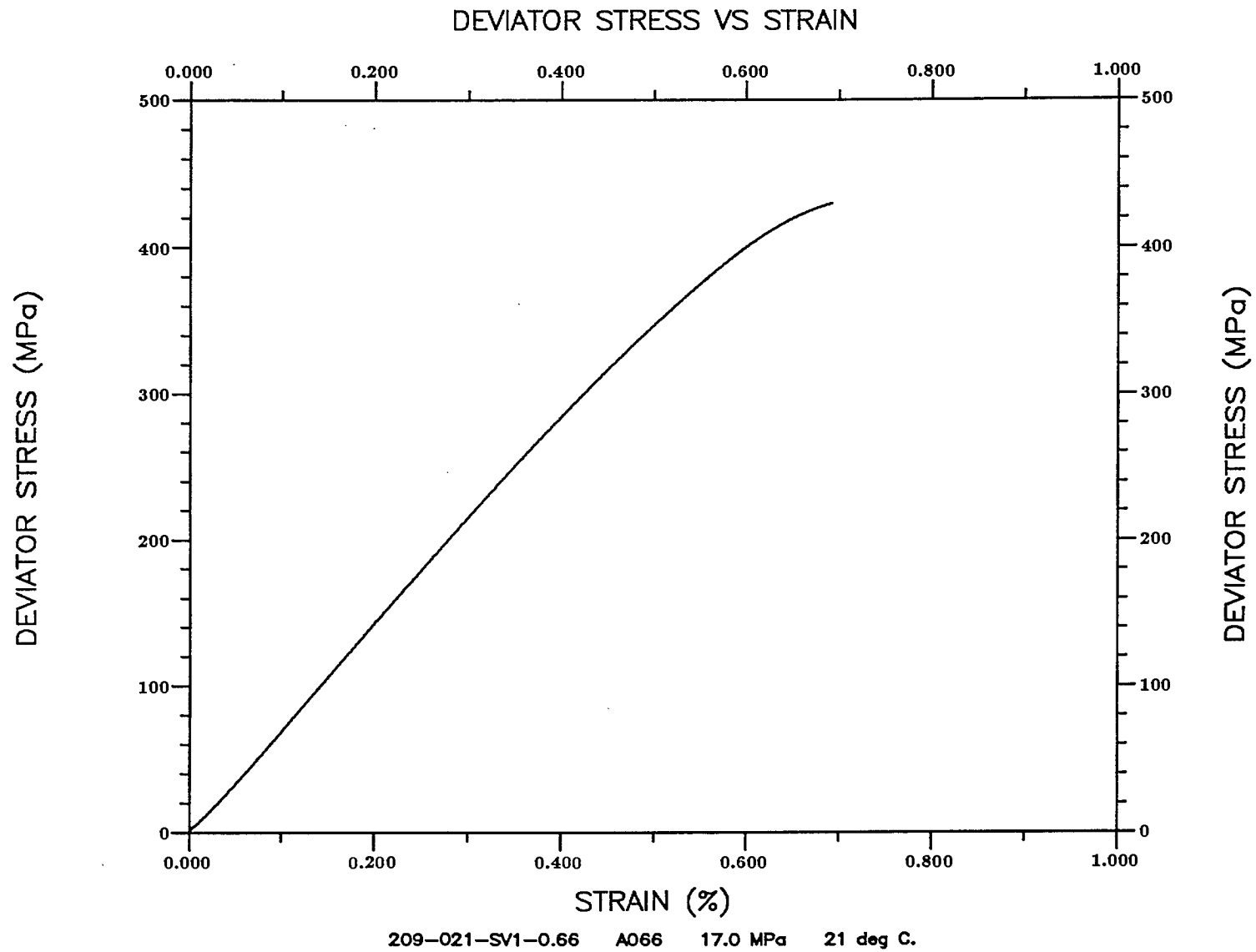


Figure A.7. Specimen 209-021-SV1-0.66 ($\sigma_3 = 17.0$ MPa, temperature = 21° C)

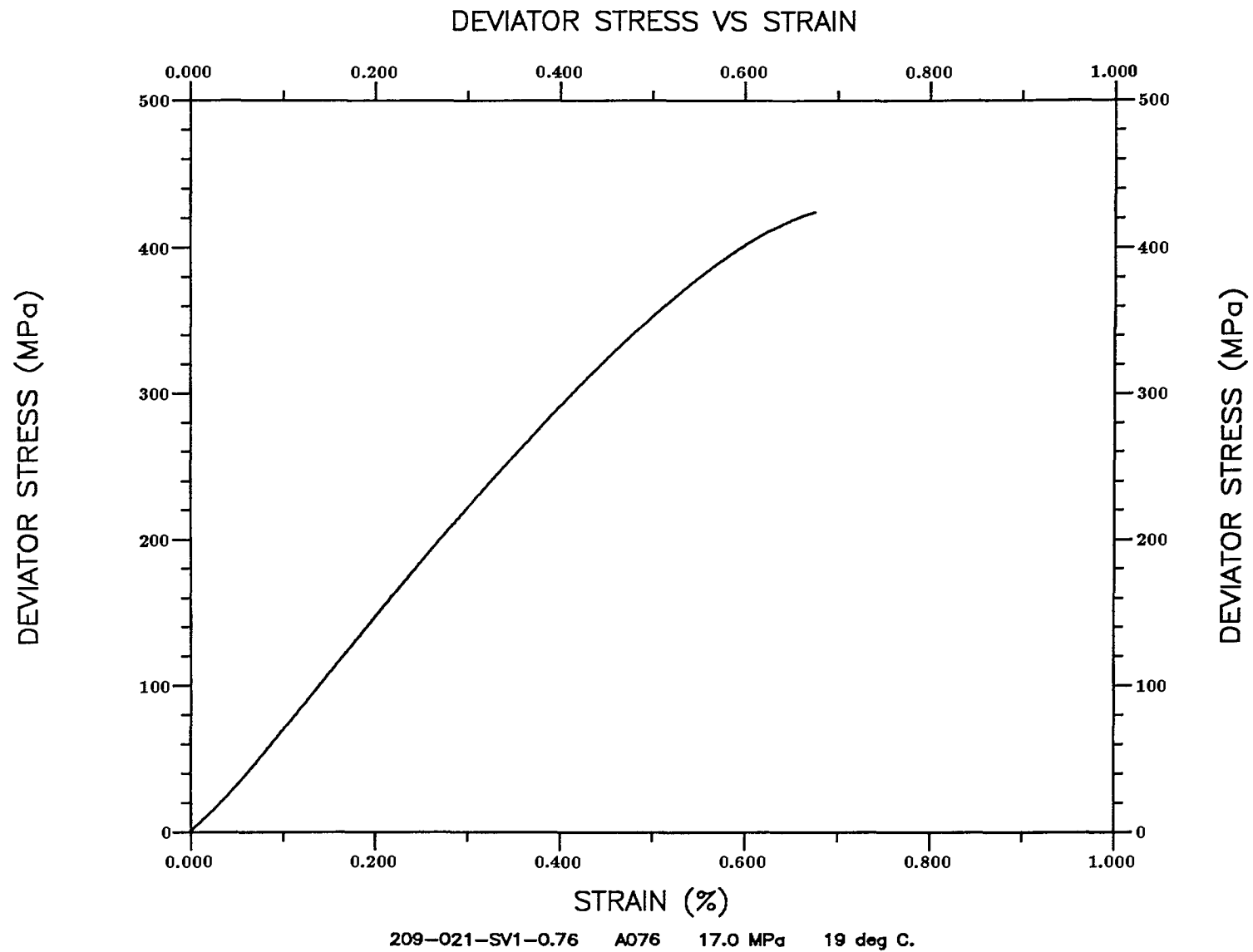


Figure A.8. Specimen 209-021-SV1-0.76 ($\sigma_3 = 17.0$ MPa, temperature = 19° C)

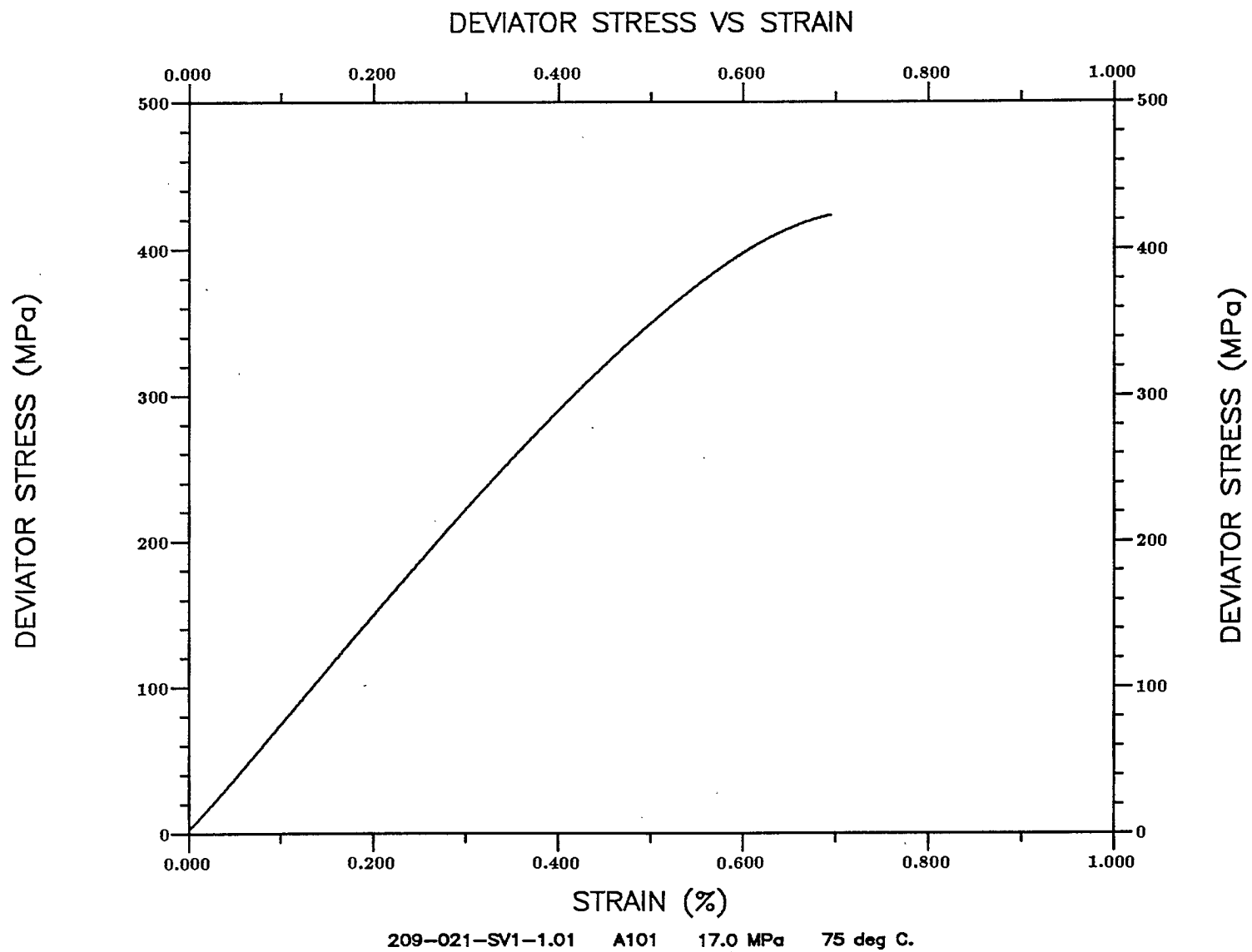


Figure A.9. Specimen 209-021-SV1-1.01 ($\sigma_3 = 17.0$ MPa, temperature = 75° C)

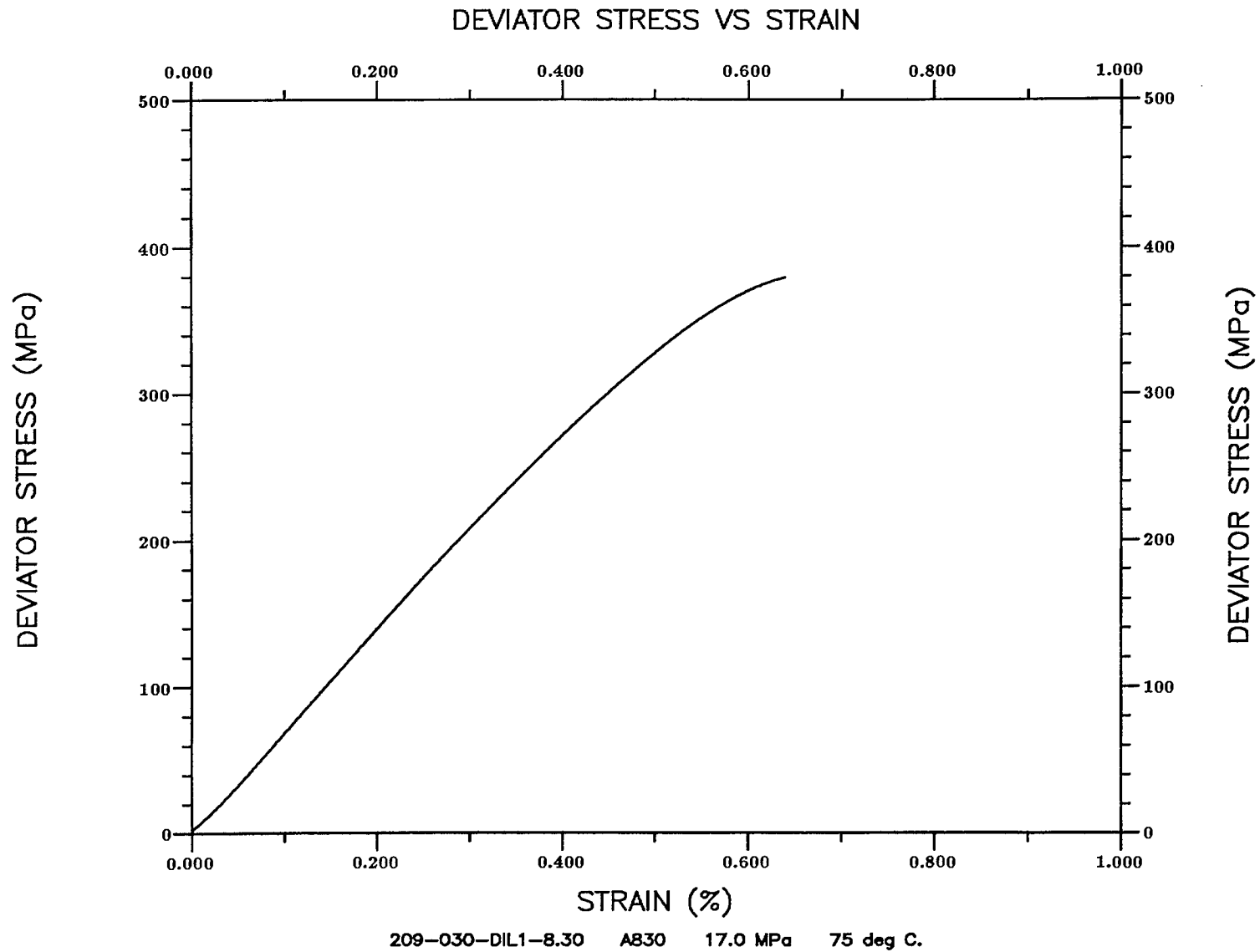


Figure A.10. Specimen 209-030-DIL1-8.30 ($\sigma_3 = 17.0$ MPa, temperature = 75° C)

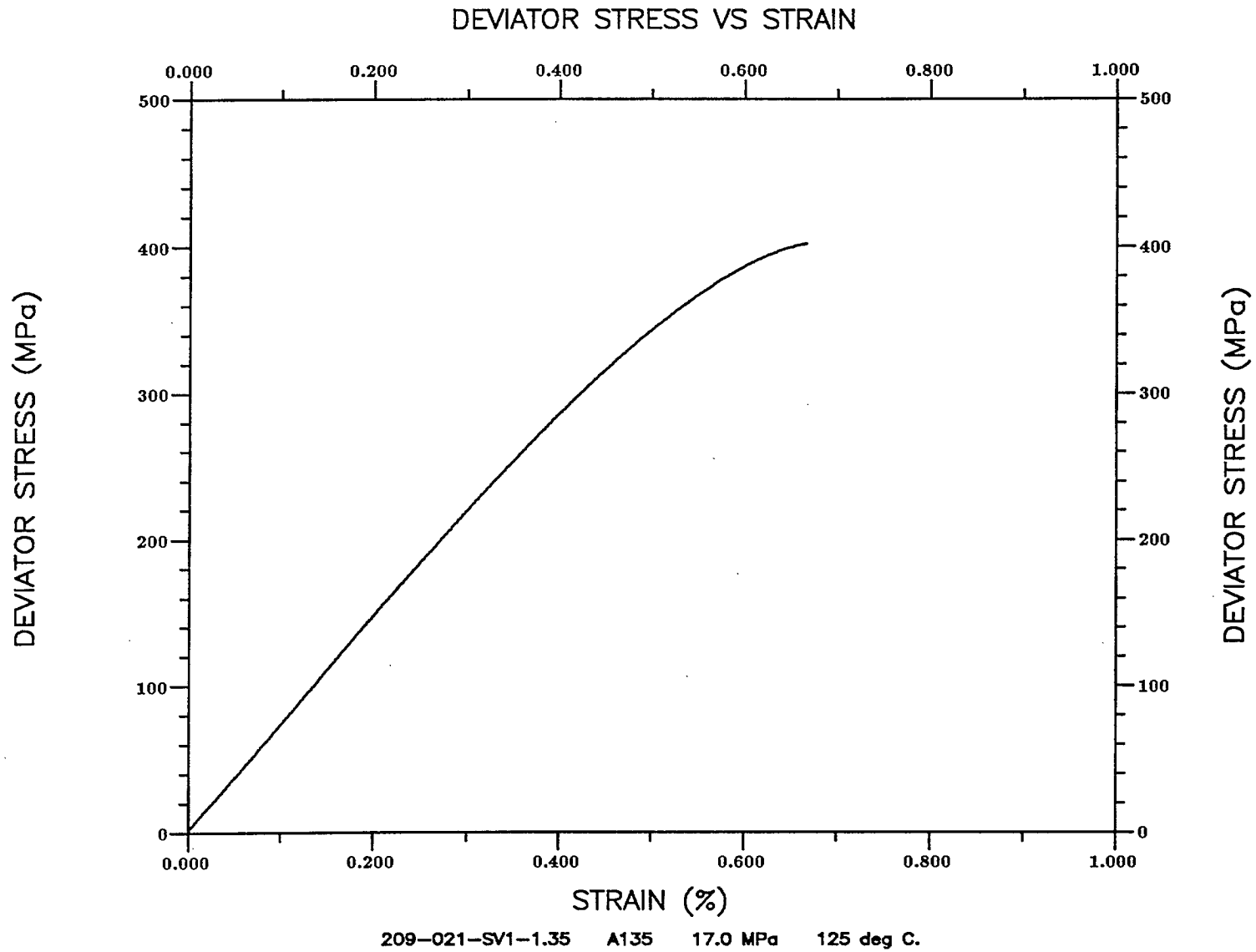


Figure A.11. Specimen 209-021-SV1-1.35 ($\sigma_3 = 17.0$ MPa, temperature = 125° C)

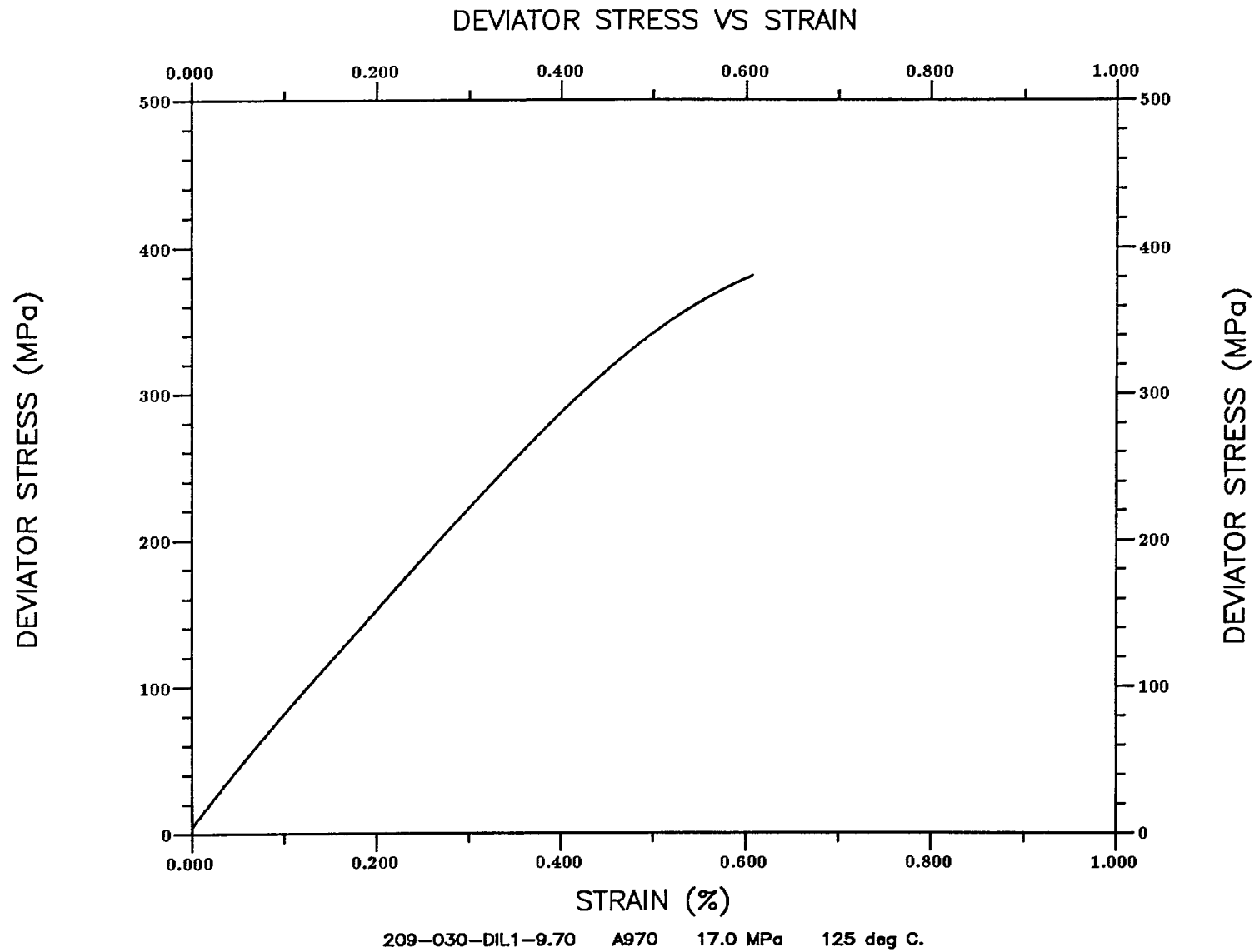


Figure A.12. Specimen 209-030-DIL1-9.70 ($\sigma_3 = 17.0$ MPa, temperature = 125° C)

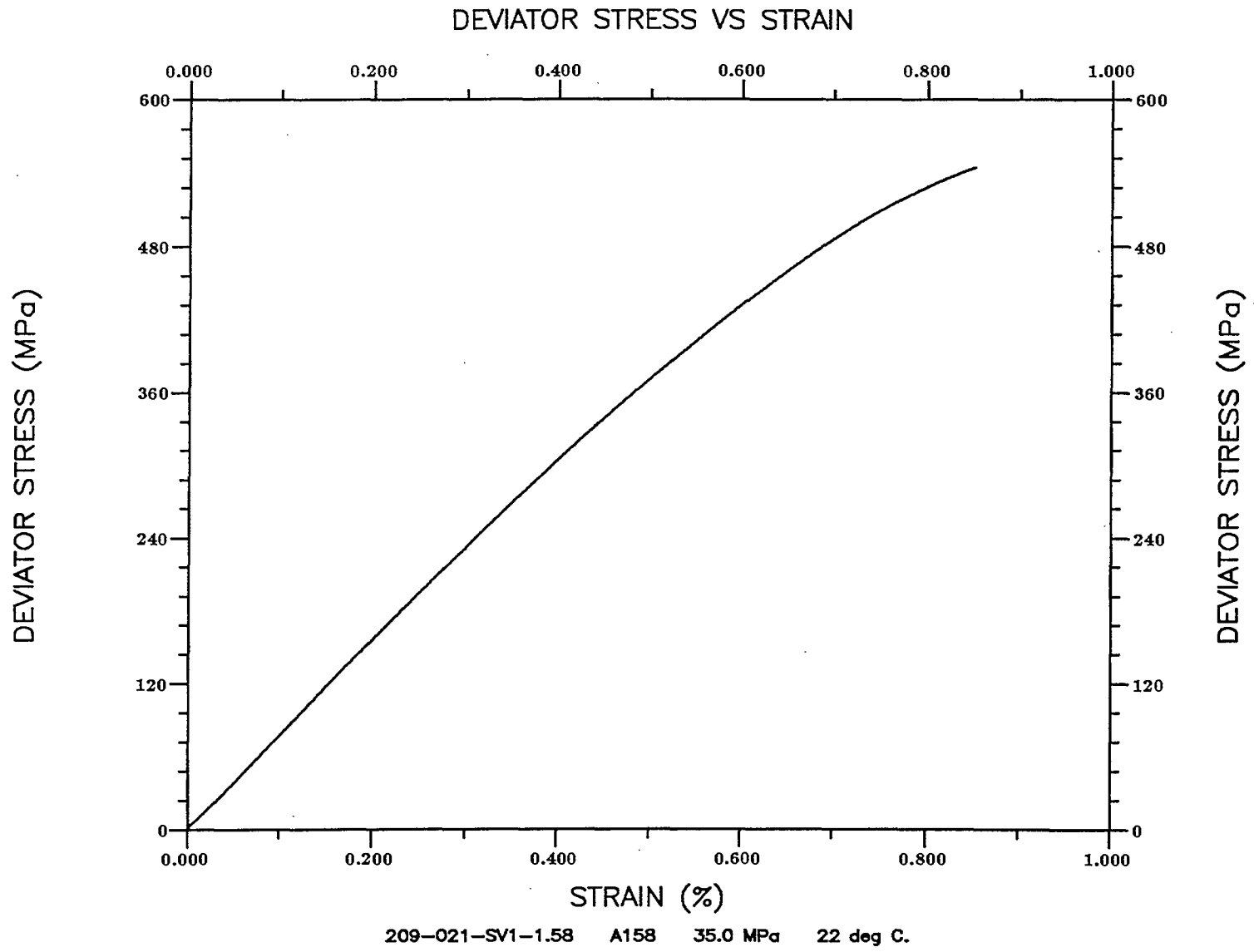


Figure A.13. Specimen 209-021-SV1-1.58 ($\sigma_3 = 35.0$ MPa, temperature = 22° C)

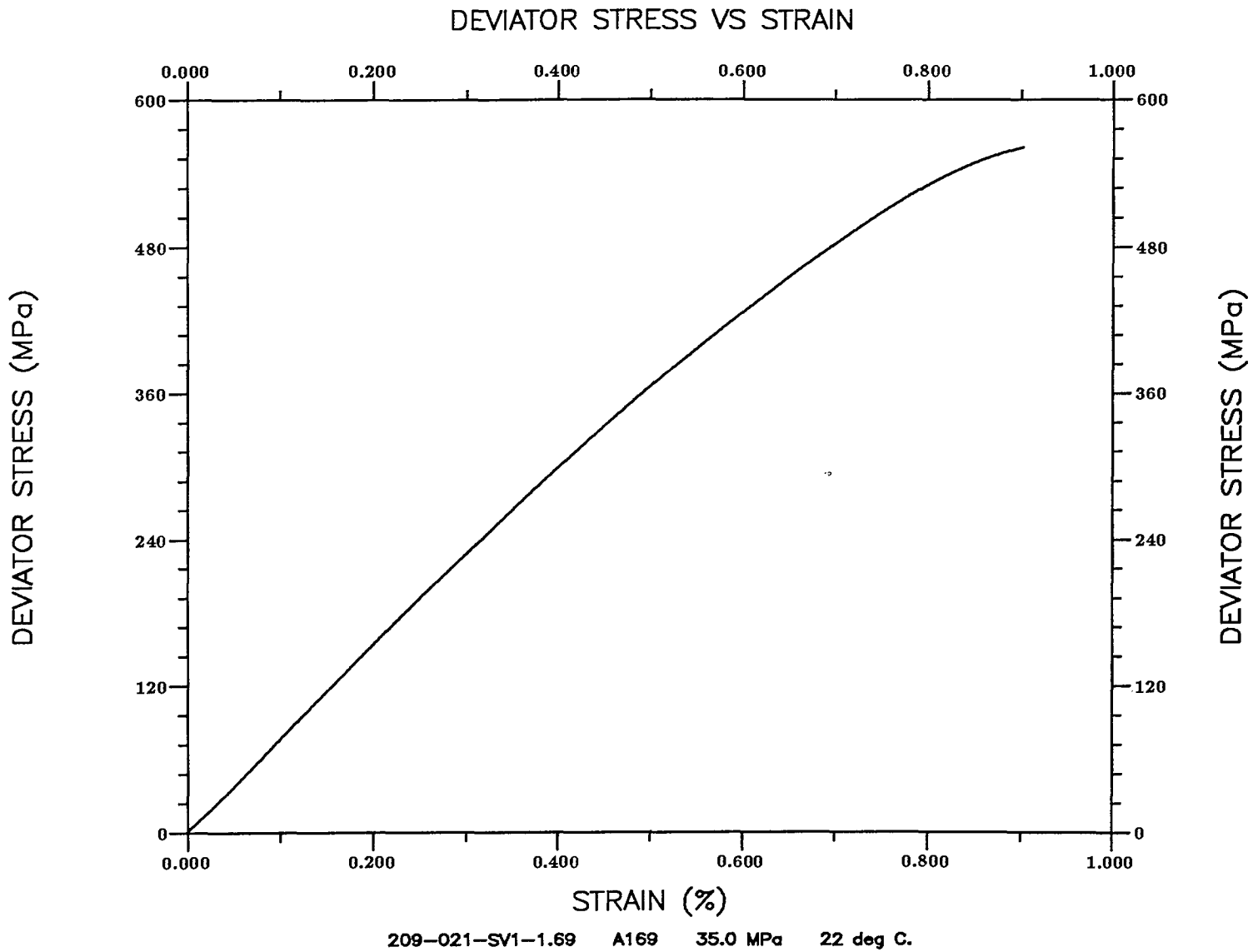


Figure A.14. Specimen 209-021-SV1-1.69 ($\sigma_3 = 35.0$ MPa, temperature = 22° C)

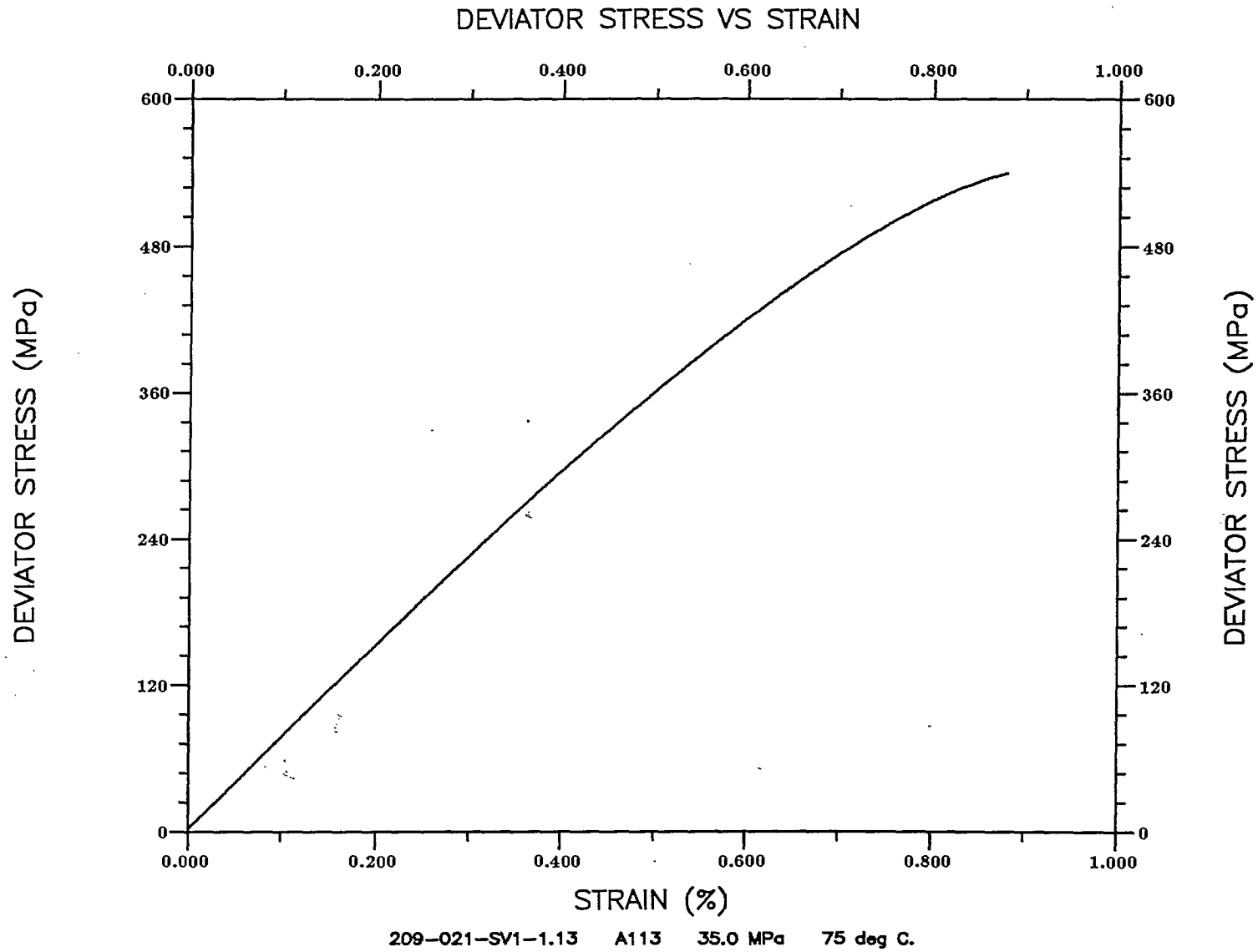


Figure A.15. Specimen 209-021-SV1-1.13 ($\sigma_3 = 35.0$ MPa, temperature = 75° C)

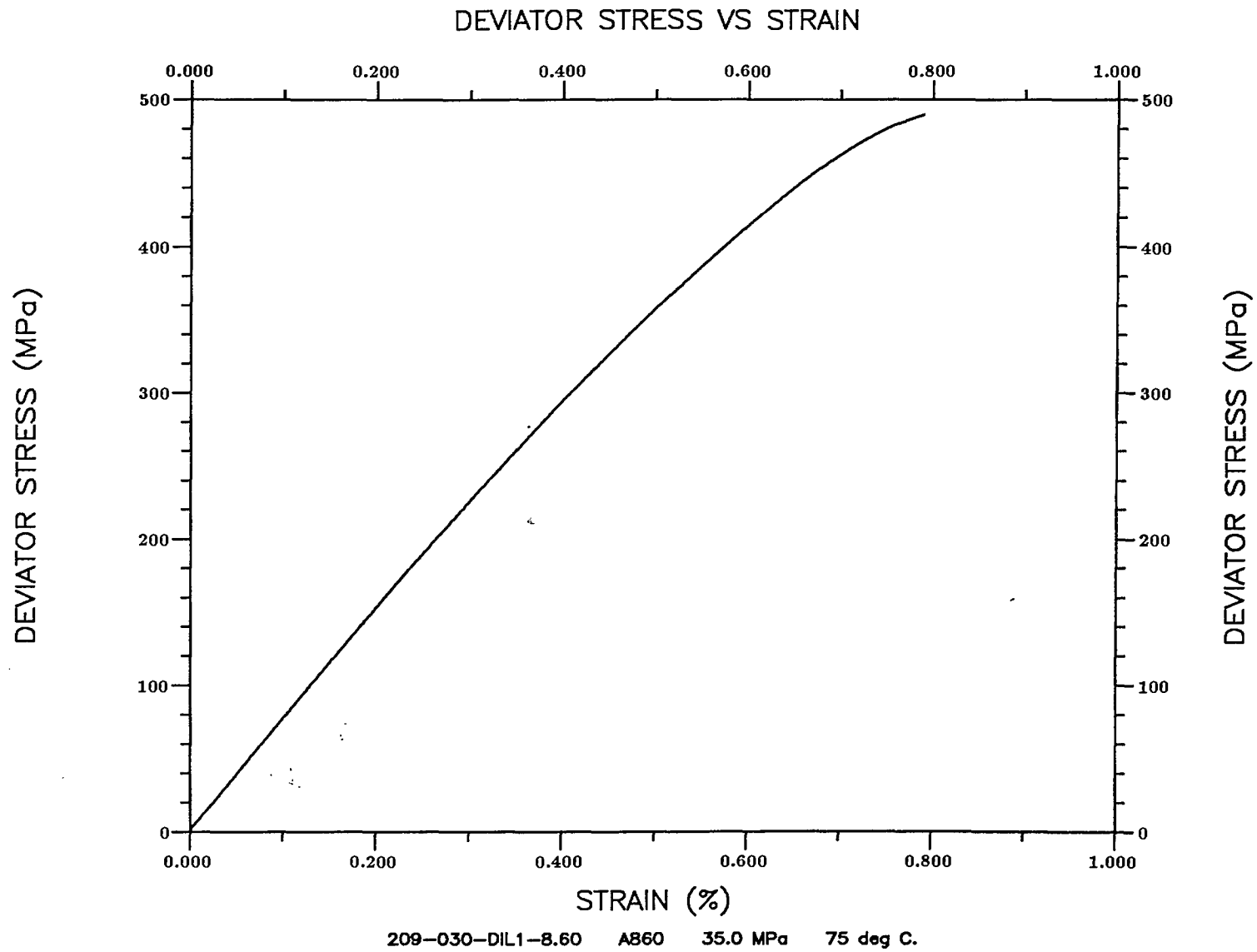


Figure A.16. Specimen 209-030-DIL1-8.60 ($\sigma_3 = 35.0$ MPa, temperature = 75° C)

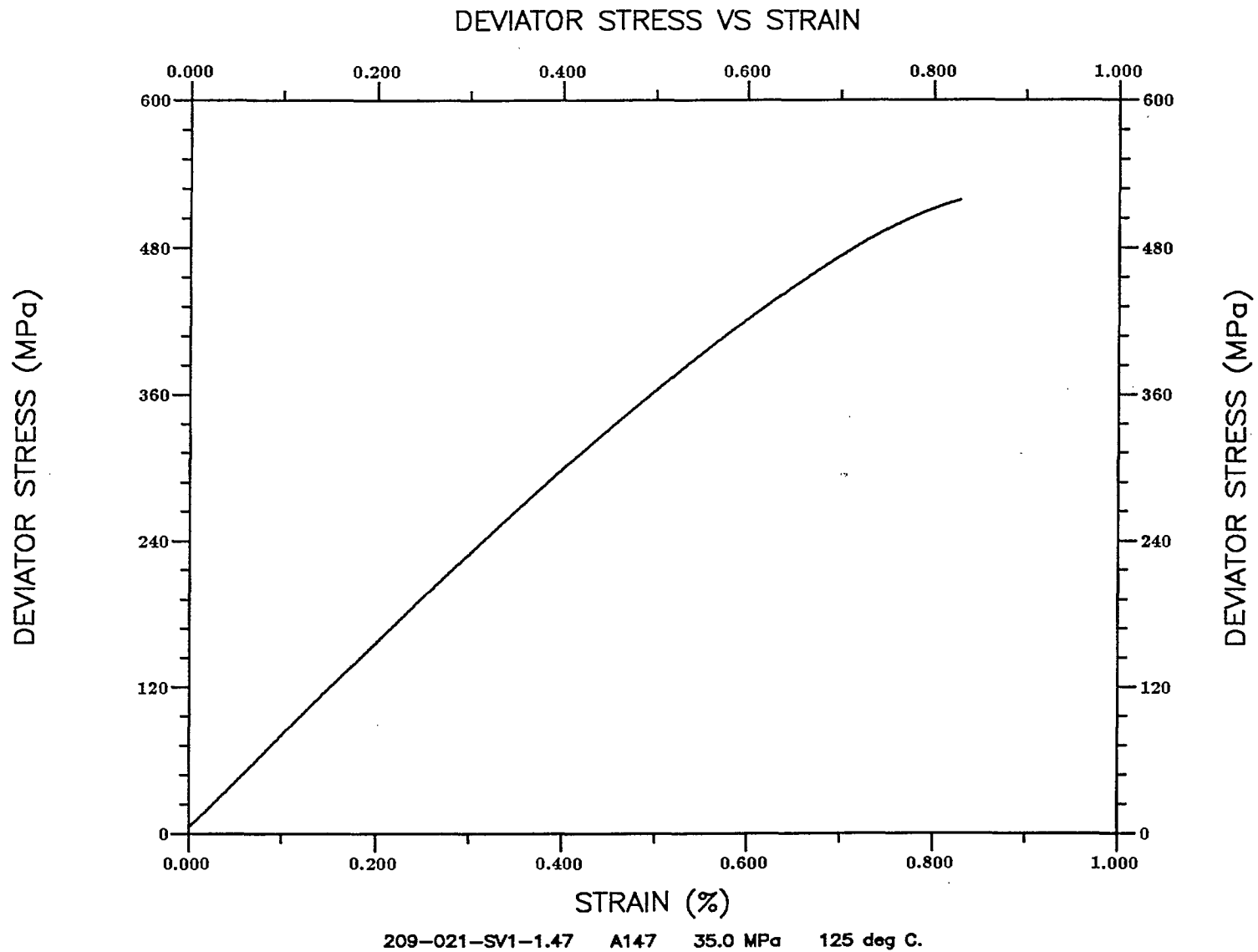


Figure A.17. Specimen 209-021-SV1-1.47 ($\sigma_3 = 35.0$ MPa, temperature = 125° C)

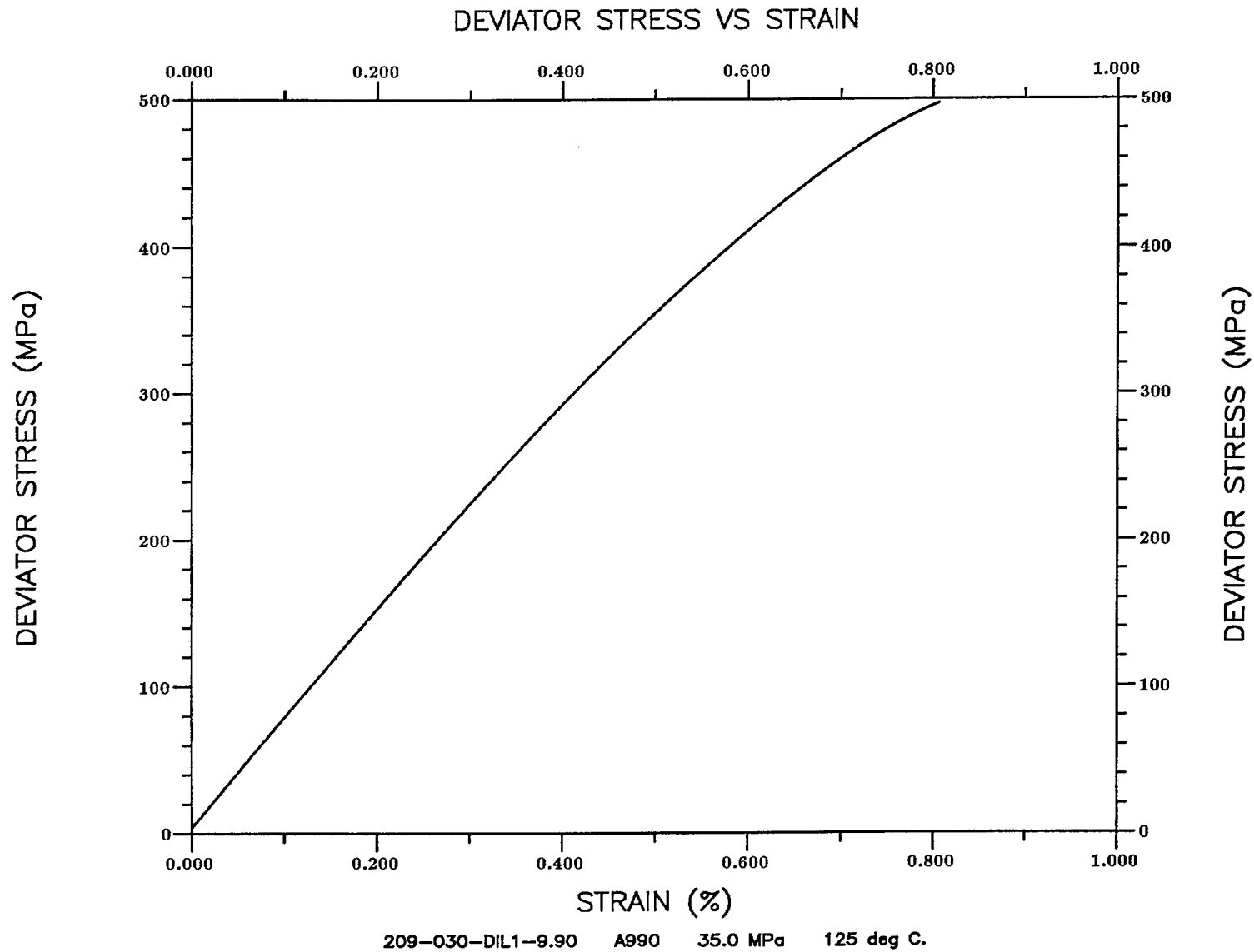


Figure A.18. Specimen 209-030-DIL1-9.90 ($\sigma_3 = 35.0$ MPa, temperature = 125° C)

